**ISTANBUL TECHNICAL UNIVERSITY ★ GRADUATE SCHOOL OF SCIENCE ENGINEERING AND TECHNOLOGY**

# EVALUATION OF INTERACTIONS BETWEEN SKOV3 CELLS AND HER2 TARGETED MONOCLONAL ANTIBODY WITH QUARTZ CRYSTAL MICROBALANCE WITH DISSIPATION AS A NOVEL APPROACH

**M.Sc. THESIS**

**Hatice EKER**

**Department of Molecular Biology Genetics and Biotechnology**

**Molecular Biology Genetics and Biotechnology Programme**

**JULY 2020**

**ISTANBUL TECHNICAL UNIVERSITY ★ GRADUATE SCHOOL OF SCIENCE ENGINEERING AND TECHNOLOGY**

# EVALUATION OF INTERACTIONS BETWEEN SKOV3 CELLS AND HER2 TARGETED MONOCLONAL ANTIBODY WITH QUARTZ CRYSTAL MICROBALANCE WITH DISSIPATION AS A NOVEL APPROACH

**M.Sc. THESIS**

**Hatice EKER**
**(521171109)**

**Department of Molecular Biology Genetics and Biotechnology**

**Molecular Biology Genetics and Biotechnology Programme**

**Thesis Advisor: Prof. Dr. Fatma Neşe KÖK**
**Thesis Co-Advisor: Dr. Turgay KAÇAR**

**JULY 2020**

**ISTANBUL TEKNİK ÜNİVERSİTESİ ★ FEN BİLİMLERİ ENSTİTÜSÜ**

# DİSİPASYONLU KUVARS KRİSTAL MİKROTERAZİ İLE SKOV3 HÜCRELERİ VE HER2 HEDEFLİ MONOKLONAL ANTİKOR ARASINDAKİ ETKİLEŞİMLERİN DEĞERLENDİRİLMESİ

**YÜKSEK LİSANS TEZİ**

**Hatice EKER**
**(521171109)**

**Moleküler Biyoloji Genetik ve Biyoteknoloji Anabilim Dalı**

**Moleküler Biyoloji Genetik ve Biyoteknoloji Programı**

**Tez Danışmanı: Prof. Dr. Fatma Neşe KÖK**
**Eş Danışman: Dr. Turgay KAÇAR**

**TEMMUZ 2020**

Hatice Eker, a M.Sc. student of İTU Graduate School of Science Engineering and Technology student ID 521171109, successfully defended the thesis/dissertation entitled "EVALUATION OF INTERACTIONS BETWEEN SKOV3 CELLS AND HER2 TARGETED MONOCLONAL ANTIBODY WITH QUARTZ CRYSTAL MICROBALANCE WITH DISSIPATION AS A NOVEL APPROACH", which she prepared after fulfilling the requirements specified in the associated legislations, before the jury whose signatures are below.

| | | |
|---|---|---|
| **Thesis Advisor :** | **Prof. Dr. Fatma Neşe KÖK**<br>İstanbul Technical University | ..... |
| **Co-advisor :** | **Dr. Turgay KAÇAR**<br>Arven Pharmaceuticals | ..... |
| **Jury Members :** | **Prof. Dr. Ayten Yazgan Karataş**<br>Istanbul Technical University | ..... |
| | **Prof. Dr. Zeynep Petek Çakar**<br>Istanbul Technical University | ..... |
| | **Dr. Ülkü Yılmaz Şahin**<br>Arven Pharmaceuticals | ..... |

**Date of Submission : 4 June 2020**
**Date of Defense : 21 July 2020**

***To them who know themselves,***

## FOREWORD

First, I would like to thank my supervisor, Prof. Dr. Fatma Neşe KÖK with all my respect, for giving me the possibility to work in her research group, the extensive freedom in trying various experiments on my own under her tolerant guidance and support. Her critical way of thinking strengthened my scientific background and enlightened my way throughout my studies, and every time will illuminate my academic future.

I want to thank Dr. Turgay KAÇAR as my co-supervisor and Arven Pharmaceuticals, for their help and support in my study.

I want to express my thanks to my dear jury members Prof. Dr. Ayten YAZGAN KARATAŞ, Prof. Dr. Zeynep Petek ÇAKAR, and Dr. Ülkü YILMAZ ŞAHİN for accepting to be my jury member.

I want to express my thanks to Dr. Abdulhalim KILIÇ for guiding and helping me in designing experiments that were very valuable for me to progress my thesis.

I want to express my thanks to Süleyman ÇELİK for guiding and helping me with the experiments.

I would also like to kindly thank my lab friends, Ayşe Buse ÖZDABAK, Burcu DOYMUŞ, Canan ÇİL, Ceren KUTLU KAYA, Şebnem SEHERLER, Elifcan ZENGİN who have been helpful and friendly with me. It was a pleasure to work with them.

I am grateful to my devoted family for their love, support, encouragement, and understanding.

Last, I am grateful to my university, my program, and Research Center (MOBGAM) for providing me these opportunities.

July, 2020 Hatice EKER

**TABLE OF CONTENTS**

**Page**

## ABBREVIATIONS

**ADCC** : Antibody-Dependent Cell Mediated Cytotoxicity
**BSA** : Bovine Serum Albumin
**CDC** : Complement-Dependent Cytotoxicity
**CDRs** : Complementarity-Determining Regions
**DMEM** : Dulbecco's Modified Eagle Culture Medium
**EGF** : Epidermal Growth Factor
**EGFR** : Epidermal Growth Factor Receptor
**EDTA** : Ethylene Diamine Tetra Acetic acid
**ELISA** : Enzyme-Linked ImmunoSorbent Assay
**Fab** : Antigen-Binding Fragment
**Fc region** : Fragment Crystallizable Region
**FBS** : Fetal Bovine Serum
**FRs** : Framework Regions
**HEPES** : 4-(2-hydroxyethyl)-1-piperazineethanesulfonic acid
**Ig** : Immunoglobulin
**mAb** : Monoclonal Antibody
**MOA** : Mechanism of action
**OD** : Optical Density
**PBS** : Phosphate buffered saline
**QCM** : Quartz Crystal Microbalance
**QCM-D** : Quartz Crystal Microbalance with Dissipation Monitoring
**SKOV3** : Human Ovary Adenocarcinoma Cells
**SPR** : Surface Plasmone Resonance
**TIR** : Total Internal Reflection ()
**UV** : Ultraviolet

**SYMBOLS**

| | |
|---|---|
| **Δf** | : Frequency Change |
| **ΔD** | : Dissipation Change |
| **μ** | : micro |
| **M** | : Molarite |
| **$CO_2$** | : Carbon Dioxide |
| **kDa** | : KiloDalton |
| **nm** | : nanometer |

**LIST OF FIGURES**

**Page**

## EVALUATION OF INTERACTIONS BETWEEN SKOV3 CELLS AND HER2 TARGETED MONOCLONAL ANTIBODY WITH QUARTZ CRYSTAL MICROBALANCE WITH DISSIPATION AS A NOVEL APPROACH

## SUMMARY

There has been an exponential growth in the biotechnology industry which is resulted in the presence of more than hundreds of biotechnological molecules in several therapeutic areas. Biotechnological drugs differ in many ways from more common chemical drugs. For instance, chemical drugs are small and stable molecules that are produced by well-defined processes with chemical synthesis, but biopharmaceutical products are large and complex biomolecules with a heterogeneous structure. Unlike chemical drugs that are not or barely sensitive to process changes, biopharmaceuticals are tremendously sensitive to process changes, and they are prepared by using alive systems that modified using recombinant DNA technology, mainly bacteria, and mammalian cells.

The largest group of biopharmaceuticals is monoclonal antibodies (mAbs). mAbs are presently utilized in many therapeutic areas for cancer therapies, cardiovascular diseases, inflammatory diseases, infections, organ transplantations, respiratory diseases, and ophthalmologic diseases.

Each step from the protein expression to the final product in the mAb production processes should be robustly controlled in order to assure quality and consistency. Furthermore, the definition and profiling of critical quality properties, including the structure of mAb, post-translational modifications in the structure, the binding activity, and biomolecular and cellular level functions is required.

In this study, the aim is to develop a label-free method to evaluate the bioactivity of mAb-based biotechnological drugs in short duration. For this purpose, Quartz Crystal Microbalance with Dissipation Monitoring (QCM-D) was selected for real-time, label-free bioactivity evaluation of HER2 targeted mAb on SKOV3 (human ovary adenocarcinoma) cells. Both frequency (f) and dissipation (D) values are affected by the changes in cell-surface interface, e.g. viscoelasticity, cell movements and/or cell reorganizations. To monitor these changes, first measurement parameters were optimized and then the change in signal as a result of mAb treatment was monitored in QCM-D. Interpretation of QCM-D data was also complemented with the examination of changes in cell morphology under the fluorescence microscope after the fixation and staining protocol.

Before QCM-D studies, measurement conditions were optimized using different initial cell numbers, incubation conditions, and incubation time, and cell distributions were analyzed by cell staining under fluorescence microscope. In order to avoid cell stacking, the most suitable cell amount was determined as $0.5x10^5$ cells for drug trials. To eliminate the interference that may be originated from serum proteins, drug trials were conducted in serum-free media. To see the effect of serum-free media on cells,

the cells were fixed and stained, and no significant differences were observed between cell morphologies in different media conditions. Before drug trials, cells were incubated for 15, 20, and 24 hours after seeding to determine the most suitable incubation time. To allow cells to completely spread to surface, incubation time after seeding was determined as 24 hours.

For drug trials, when the stable baseline for both frequency and dissipation at the third harmonics was obtained, media containing HER2-mAb was pumped to the measurement chamber until the whole chamber was filled and the cells were incubated with HER2-mAb under no-flow conditions. The response of SKOV-3 cells to HER2-mAb at different concentrations, i.e. 40, 80, 120, and 160 µg/mL were analyzed.

While there was noticeable increase in frequency, a characteristic decrease in dissipation was observed in drug treatment experiments. There was almost no change in QCM-D signals in control experiments in which no drug was used. In addition to those noticeable changes in $\Delta f$ and $\Delta D$ signals, drug concentration also caused significant change in acoustic ratio ($\Delta D/\Delta f$) values which gives information about the viscoelastic properties of the cell layer.

To visualize the cell morphologies and spreading, cells were stained with the Phalloidin dye acting on the cytoskeleton. The effect of the drug on the cell morphology becomes visible when 40 µg/mL drug was used, and intensity was more pronounced as concentration increased. When the morphology of the drug-treated cells compared to the control cells, a significant effect on the cell shapes can be observed. While the shape of the control cells was smooth, the cell membranes of the drug-treated cells become more curled. In addition, the edges of the cells incubated with the drug seem to be more intensely stained. This increase in intensity concentrated on specific points can be explained by the increased concentration of actin filaments at the cell edges. Actin filaments are very dynamic, so binding of the drug to SKOV3 cells may lead to increase actin filament concentration and change the distribution of actin filaments around the cell edges. These reorganizations of actin filaments would cause an increase in cell rigidity and this explains the decrease in dissipation values in QCM-D signals.

In conclusion, both the QCM-D and fluorescent microscopy images showed that HER2-mAb binding triggers the change in morphology of the cells, and the changes in QCM-D signal can be used to design label-free, real-time novel bioactivity assays for biopharmaceuticals.

# YENİ BİR YAKLAŞIM OLARAK DİSİPASYONLU KUVARS KRİSTAL MİKROTERAZİ İLE SKOV3 HÜCRELERİ VE HER2 HEDEFLİ MONOKLONAL ANTİKOR ARASINDAKİ ETKİLEŞİMLERİN DEĞERLENDİRİLMESİ

## ÖZET

Son yıllarda biyoteknoloji alanında meydana gelen hızlı gelişmeler, biyoteknolojik ilaçların farmasötik endüstrisindeki oranını ve değerini önemli derecede arttırmıştır. Biyoteknolojik moleküller sağlamış oldukları avantajlarla yeni biyoteknolojik ilaçların geliştirilmesi konusunda önemli bir ivme yaratmakta ve biyoteknolojik yöntemlerle üretilen aktif olarak kullanılan ve ruhsatlanan ilaçların sayısı giderek artmaktadır. Biyolteknolojik ilaçlar kanser, kalp hastalıkları ve diyabet gibi toplumda yüksek oranlarda görülen hastalıklar başta olmak üzere birçok değişik sağlık sorununu içeren yaklaşık olarak 200 hastalığın tedavisi için geliştirilen yeni ilaçların büyük bir kısmını oluşturmaktadır. Bu ilaçların daha yaygın kullanılan kimyasal ilaçlarla aralarında kritik farklılıklar vardır. Kimyasal ilaçlar, formülleri bilinen, stabil bir yapıya sahip ve kimyasal sentez ile üretilen küçük moleküller iken, biyofarmasötik ürünler heterojen bir yapıya sahip olan karmaşık ve büyük biyomoleküllerdir. Üretim esnasındaki proses değişikliklerine duyarlı olmayan veya çok az duyarlı olan kimyasal ilaçların aksine, biyofarmasötikler proses değişikliklerine karşı son derece duyarlıdır. Biyofarmasötiklerin büyük çoğunluğu rekombinant DNA teknolojisi ile canlı sistemler, özellikle bakteri ve memeli hücreleri, kullanılarak üretilir.

Monoklonal antikorlar (mAb), biyofarmasötiklerin en büyük sınıfıdır ve şu anda kanser, enflamatuar hastalıklar, kardiyovasküler hastalıklar, organ nakli, enfeksiyonlar, solunum hastalıkları ve oftalmolojik hastalıkların tedavisinde kullanılmaktadır. Tümör hücreleri yüksek hızda çoğalmalarına ya da anormal yapıda olmalarına rağmen hastanın kendi hücreleri olduğu için genellikle bağışıklık sistemi tarafından tanınıp hedeflenemez. Çok geniş çerçeveden bakılacak olursa monoklonal antikorlar vücuttaki tümör hücrelerini veya anormal hücreleri işaretlemek için kullanılıp, bağışıklık sistemi hücrelerinin bu anormal hücrelere saldırmasını sağlar.

mAb üretiminin kalitesini ve kalitenin devamlılığını garanti etmek için protein ifadesinden depolama fazına kadar olan her süreç adımı iyi kontrol edilmeli ve analizleri yapılmalıdır. Monoklonal antikorların protein yapılarının analiz edilmesi, translasyon sonrası değişikliklerin kontrolünün sağlanması, bağlanma aktivitesi ve biyomoleküler ve hücresel fonksiyonlar dahil kritik kalite özellik seviyelerinin tanımlanması gerekmektedir.

Bu çalışmada amaç, mAb gibi biyoteknolojik ilaçların biyoaktivitesini kısa sürede değerlendirmeyi sağlayan ve etiket gerektirmeyen yeni bir analiz yönteminin geliştirilmesidir. Bu amaçla Disipasyon İzlemeli Kuvars Kristal Mikrotekrazi (QCM-D) yöntemi model bir monoklonal antikorun biyoaktivitesinin gerçek zamanlı ve etiketsiz bir şekilde değerlendirilebilmesi için kullanılmıştır. Seçilen mAb'ın HER2 reseptörüne bağlanması dikkate alınarak, bu reseptörlerin yüksek miktarda bulunduğu

insan yumurtalık adenokarsinomu (SKOV3) hücreleri kullanılmıştır. QCM-D tekniği, sensör yüzeyine tutunup yayılan hücre katmanının hem kütle miktarının hem de viskoelastik özelliklerinin karakterizasyonunun yapılmasını sağladığı için tercih edilmiştir. QCM-D yüzey-hücre arayüzeyindeki değişikliklere hassas olduğu için hücre hareketleri ve/veya hücre reorganizasyonda meydana gelen değişiklikler hem frekans (f) hem de disipasyon (D) değerlerinde değişikliklere yol açar. QCM-D sinyallerindeki frekans değişimi (Δf) kütle değişimini yansıtırken, disipasyon değişikliği (ΔD) viskoelastik özelliklerle ilişkilidir. Akustik oran (ΔD / Δf) ise her bir frekans değişimi başına disipasyon değişimini göstermekte olup sensör yüzeyindeki katmanın viskoelastik özelliği hakkında detaylı bir bilgi vermektedir. Bu şekilde ilacın bağlanması sonrası hücrede meydana gelen değişiklikler etiketleme olmadan gerçek zamanlı izlenebilmiş olur.

Çalışmamızda öncelikle QCM-D deneylerinde kullanılan ilacın hücreler üzerindeki etkisini net bir şekilde görebilmek için çeşitli optimizasyonlar yapılmıştır. İlk olarak ilaç denemelerinde kullanılacak hücre sayısı ve hücrelerin inkübasyon koşulları ve inkübasyon süresi optimize edilmiştir. Hücre sayısı hücreler fikse edilip boyandıktan sonra floresan mikroskobu altında hücrelerin dağılımları ve konsantrasyonu incelenerek belirlenmiştir. Yapılan incelemeler sonucunda hücrelerin birbirlerine çok yakın olmadığı, yayılmalarının ve hareketlerinin kısıtlanmadığı en uygun hücre miktarı $0.5x10^5$ hücre olarak belirlenmiştir. Serum proteinlerininin varlığı hücre bağlanma davranışını değiştirip QCM-D sinyalini ayırt etmeyi zorlaştırdığından ilaç bağlanma denemeleri serumsuz besi yeri kullanılarak gerçekleştirilmiştir. Bu nedenle hücrelerin serumsuz besi yerinde inkübe edilmesinin hücre morfolojileri üzerinde bir etkisinin olup olmadığı araştırılmıştır. Hücreler fikse edilip boyandıktan sonra morfolojilerinin incelenmesi sonucunda serumlu ve serumsuz ortamda inkübe edilen hücreler arasında önemli bir fark gözlenmemiştir. Son olarak da hücrelerin yüzeye ekildikten sonraki inkübasyon süreleri optimize edilmiştir. Bunun için hücreler sensör yüzeyine ekilip 15, 20 ve 24 saat inkübe edildikten sonra QCM-D deneylerine alınmıştır. QCM-D sinyallerindeki frekans, disipasyon ve akustik oran değişimleri incelenerek hücrelerin yüzeye tamamen yayıldığını gösteren 24 saat, inkübasyon süresi olarak belirlenmiştir.

İlaç denemeleri için, üçüncü harmoniklerde hem frekans hem de disipasyon sinyallerinde dengeye ulaşıldığında HER2 monoklonal antikoru içeren besi yeri, QCM ölçüm odası dolana kadar odacığa pompa yardımıyla gönderilmiştir. İlaçlı besi yeri QCM odacığına ulaştıktan sonra akış durdurulup hücreler HER2 reseptörüne bağlanan monoklonal antikor ile belirli bir süre boyunca inkübe edilmiştir. QCM-D çalışmalarında, SKOV-3 hücrelerinin 40, 80, 120 ve 160 ug/mL konsantrasyonlarındaki HER2 reseptörüne bağlanan mAb'a karşı tepkileri analiz edilmiştir.

İlaç denemeleri sonunda QCM-D frekans değerlerinde belirgin bir artış olurken, disipasyon sinyallerinde karakteristik bir azalma gözlenmiştir. Kontrol deneylerinin yani ilaçsız besi yeri ile inkübe edilen hücrelerin QCM-D sinyallerinde ise neredeyse hiçbir değişiklik gözlenmemiştir. Δf ve ΔD sinyallerindeki bu belirgin değişikliklere ek olarak, artan ilaç konsantrasyonu, hücrelerin viskoelastik özellikleri hakkında bilgi veren akustik oran (ΔD / Δf) değerinde de önemli bir düşüşe neden olmuştur.

İlaç deneyleri sonucunda hücre morfolojilerinde ve yayılmasında meydana gelen değişikliklerin görsel olarak da incelenebilmesi için hücreler, hücre iskeletine etki eden Phalloidin boyası ile boyanmıştır. İlacın hücre morfolojisi üzerindeki etkisi 40

ug/mL ilaç konsantrasyonunda belirgin bir şekilde fark edilirken, ilaç konsantrasyonu arttıkça bu etki daha da yoğun bir şekilde gözlenmiştir. İlaçla muamele edilen hücrelerin morfolojileri kontrol hücrelerininki ile kıyaslandığında hücre şekilleri arasında önemli farklar gözlenmiştir. Kontrol hücrelerinin şekli daha yuvarlak ve hücre zarları daha düzgün iken ilaçla inkübe edilen hücrelerin hücre zarları daha kıvrımlı bir hale gelmiştir. Ayrıca ilaç ile inkübe edilen hücrelerin kenarları daha yoğun bir şekilde boyanmış gibi görünmektedir. Bu yoğun boyanmış alanların spesifik noktalarda artış göstermesi, hücre kenarlarındaki artan aktin filament konsantrasyonu ile açıklanabilir. Aktin filamentleri son derece dinamik olduğu için, ilacın SKOV3 hücrelerine bağlanması aktin filament konsantrasyonunun artmasına ve aktin filamentlerinin hücre kenarlarındaki dağılımının değişmesine neden olmuş olabilir. Aktin filamentlerinin bu şekilde yeniden düzenlenmesi, hücrelerin daha rijid hale gelmesine ve hücrelerin hareket etmesine, yüzey üzerinde organizasyonlarını değiştirmelerine yol açmış olabilir. Hücrelerin morfolojilerindeki bu değişiklikler QCM-D sinyallerindeki değişimin nedeni de açıklamaktadır.

Sonuç olarak, QCM-D sonuçları ve floresan mikroskopi görüntüleri monoklonal antikorun SKOV3 hücrelerine bağlanmasıyla hücre morfolojileri üzerinde önemli bir değişikliğe neden olduğunu göstermektedir Bu değişiklikler gerçek zamanlı ve etiketsiz olarak QCM-D ile takip edilebilmiştir. Bu yöntem izole edilmiş reseptörlerle ve etiketleme ile yapılan bağlanma analizleri yerine, reseptörün doğal ortamında yani hücre zarında bulunduğu haliyle kullanıldığı ve etiket gerektirmeyen biyoaktivite analizlerinde QCM-D'nin kullanılabileceği gösterilmiştir.

# 1. INTRODUCTION

## 1.1 Purpose of Thesis

In this study, the aim was the development of a real-time, label-free technique to evaluate the effect of monoclonal antibody (mAb) based biotechnological drugs in a short duration. For this purpose, Quartz Crystal Microbalance with Dissipation Monitoring (QCM-D) was selected for real-time, label-free evaluation of a HER2 targeted mAb on SKOV3 (human ovary adenocarcinoma) cells. The change in viscoelastic properties at the cell-surface interface after mAb binding to HER2 receptors of SKOV3 cells was assessed by dissipation changes in QCM-D. Cell movements, cell reorganizations on the surface after mAb binding were analyzed by frequency changes in QCM-D. Evaluation of QCM-D data was also supported with the examination of changes in cell morphology under the fluorescence microscope after the fixation of the cells on the gold sensor surface and staining with different dyes.

## 1.2 Background Information

### 1.2.1 General information about antibodies

Antibodies are produced by plasma B-lymphocytes[1]. They are found in mammals as a part of the immune system to fight against the disease or foreign molecules that enter the body [2]. When an encounter with antigenic foreign molecules, i.e. pathogens or toxins, antibodies start a complex immune response [3, 4]. Antibodies are important in modern diagnostics, treatment and basic research since specific antibodies can be developed against nearly any component, from pathogens to small drug molecules [5].

There are two main groups of antibodies such as polyclonal antibodies (pAbs) and monoclonal antibodies (mAbs). pAbs are generally produced by different B cell clones directly in animals, therefore they are a mixture of heterogeneous molecules [2, 6]. Chromatographic techniques are generally used to purify pAbs from the blood of the antigen-introduced mammals [3]. Since pAb is a mixture of antibodies against an

antigen binding different epitopes, its selectivity is low due to the increased risk of cross-reaction with biomolecules that contains similar epitopes Furthermore, as the pAbs are produced from the alive mammal's blood, the source pAbs is not unlimited since the animal will eventually die [3]. To overcome these limitations, hybridoma technology had been developed to produce monoclonal antibodies (mAb) by Kohler and Milstein in 1975 [7]. This work got Nobel Prize [8] since it revolutionized the antibody production and shaped the current diagnostic applications, disease therapy, and basic research. mAbs specifically bind to single idiotype and they are produced by immortalized B-lymphocytes. Normal B-lymphocytes are entirely differentiated and cannot be maintained in the culture environment as they are. Therefore, they are fused with myeloma cells to create immortal antibody-producing cell lines which are known as hybridoma cells by the technique introduced by Kohler and Milstein called hybridization [9] (Figure 1.1).

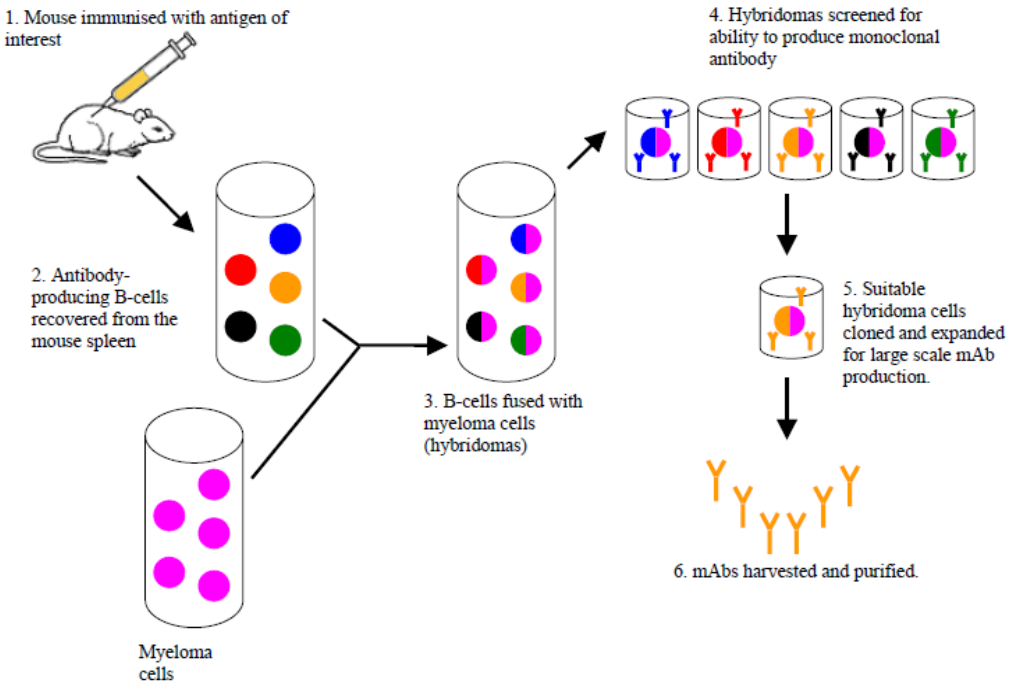


**Figure 1.1 :** Overview of mAb production[3]

### 1.2.2 Biotechnological drugs

The biotechnological industry has shown exponential growth in the biopharmaceutical area and as of today, more than five hundred biotechnology-originated molecules are in the market and more than seven thousand are under development [10]. The active substance of a biopharmaceutical is synthesized by or obtained from a living organism

to commonly replace or supplement a protein naturally produced in the body (Figure 1.3) [11, 12]. These biological agents are much more complex than conventional chemical small drug molecules in terms of their protein structure, process procedure, production technology, and action mechanisms so different strategies are used for their mass-production (Figure 1.2).

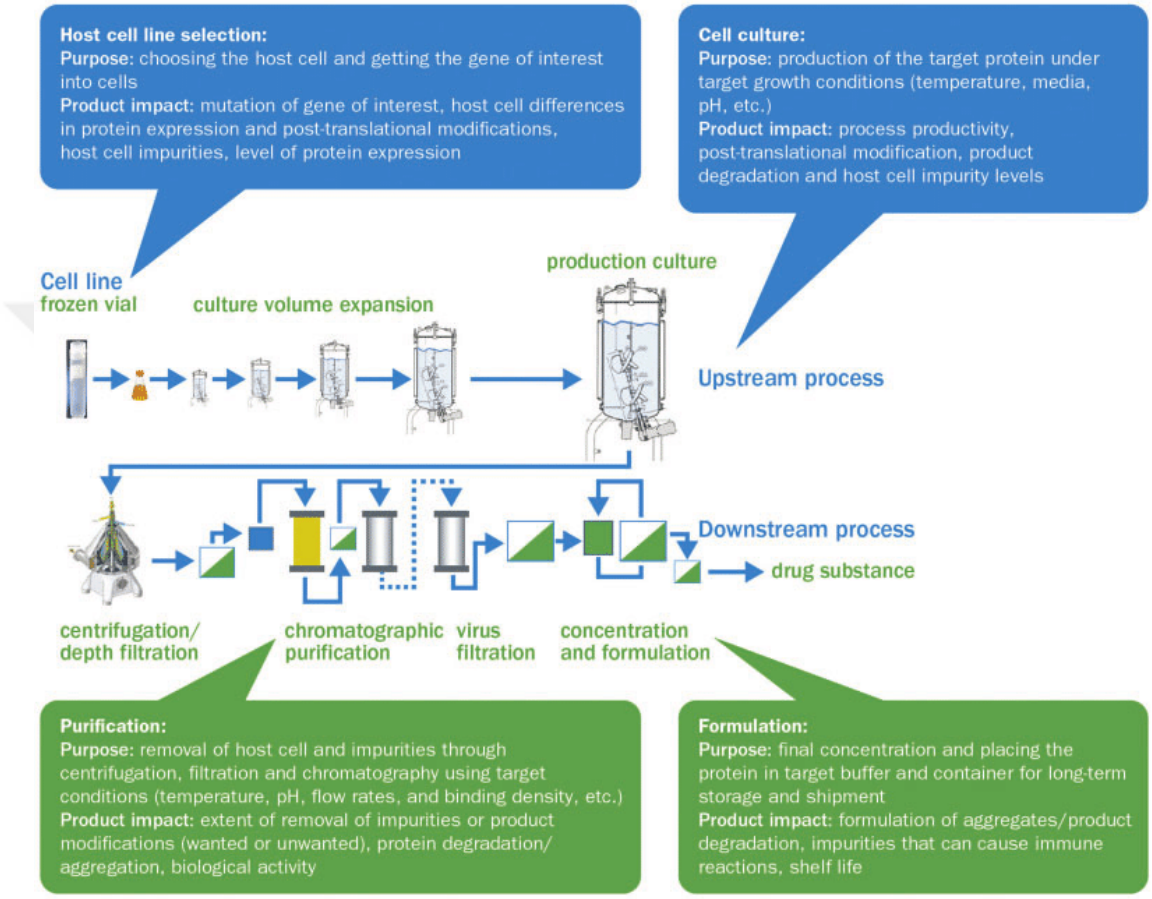


**Figure 1.2 :** The manufacturing process and manufacturing steps of biologics that affect their final characteristics [13].

Chemical drugs are small molecules produced by chemical synthesis that are not or slightly sensitive to process changes during the production step. Their chemical structure is relatively stable when compared to biotechnological drugs [14]. On the other hand, biotechnological drugs are large complex biomolecules with heterogeneous structure. Biomolecules are also extremely sensitive to the alterations in process conditions such as oxygen levels, temperature, pH, osmolality and duration [13]. Living systems, such as whole organisms, tissue cultures or genetically modified cells are needed for their production and most of them are manufactured via

recombinant DNA technology. For that, gene sequence for the target human protein is inserted mostly into mammalian cell lines for large scale production (Figure 1.3) [15].

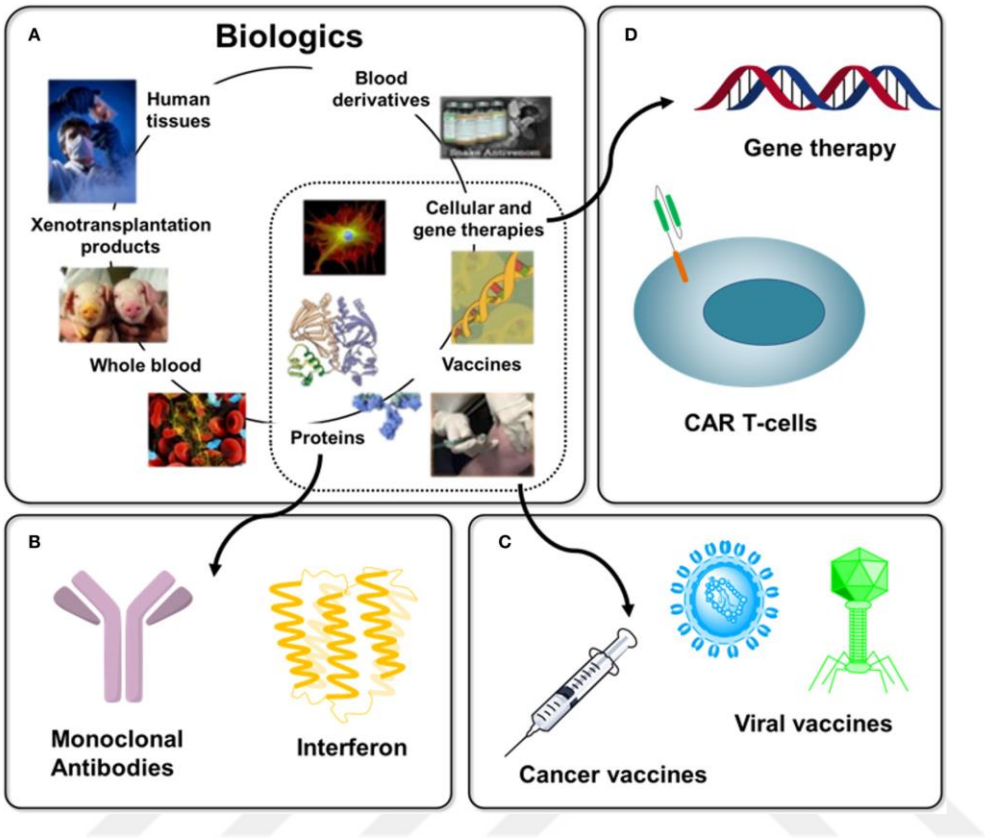


**Figure 1.3 :** Presentation of biological molecules examples that related to immunotherapy. (A) Biologics is a general expression that means any therapy created using material derived from a living system, (B) Protein-based biologics as monoclonal antibodies and interferon, (C) Cancer vaccines, (D) The emerging cell-based and gene therapies[16].

### 1.2.2.1 Monoclonal antibodies

There are five different groups of antibodies with different functions found in human serum named as IgM, IgD, IgG, IgA, and IgE (Figure 1.4) [17, 18]. Each group has its own unique functions and properties which depend on the structural differences in their heavy chains [18]. IgG is the most abundant antibody in human serum for its presence corresponds to 70-85% among the total immunoglobulin share [19]. IgGs are large heterodimeric molecules with high molecular weight (ca. 150 kDa) and their structure is composed of two kinds of polypeptide chains which are heavy (ca. 50 kDa) and the light chain (~25 kDa) as can be seen in Figure 1.5 [20].

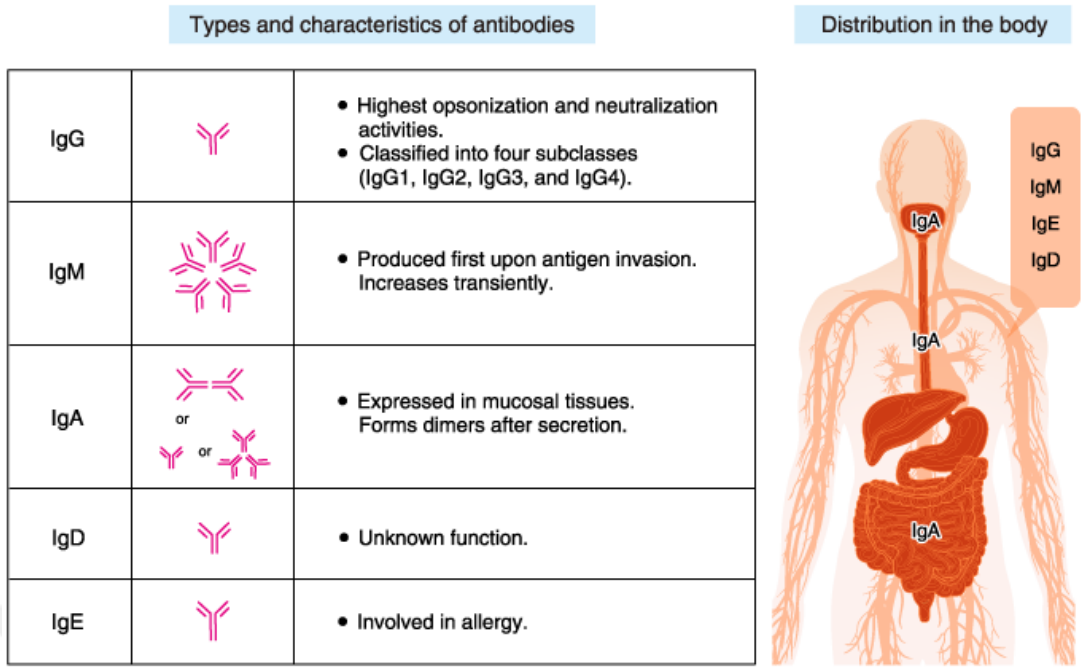


**Figure 1.4 :** Structure and characteristics of antibody isotypes[17]

The two heavy chains are generally linked by disulfide bonds forming the fragment crystallizable region (Fc region) region of the antibody. The Fc region is found in the tail region of an antibody that interacts with the surface receptor of cells called Fc receptors. The Fc part of the antibody is important to initiate the effector response by interacting with the cells of the immune system through Fc receptors. Thanks to Fc region of antibodies, the immune system is easily activated and the specificity of the effector cells is greatly increased [21].

Fab region which is another part of antibody called as antigen-binding fragment. This region contains variable regions that provide targeting and binding ability to a specific target as an antigen-binding function (Figure 1.5). It contains one constant and one variable domain of both the heavy and the light chain. In an antibody class, the Fc region is the same for all antibodies in each same species, i.e. they are not variable, much more constant [22].

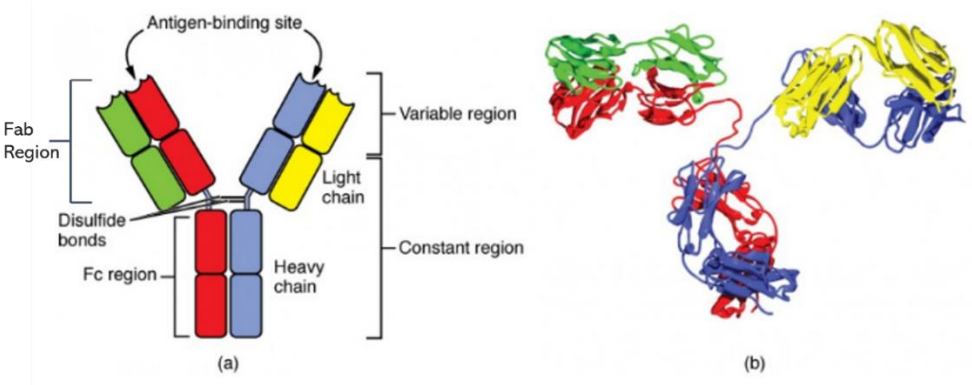


**Figure 1.5 :** (a) the classic four chain structure of a generic antibody, (b) the correlated three-dimensional (3-D) structure of the antibody IgG1[23].

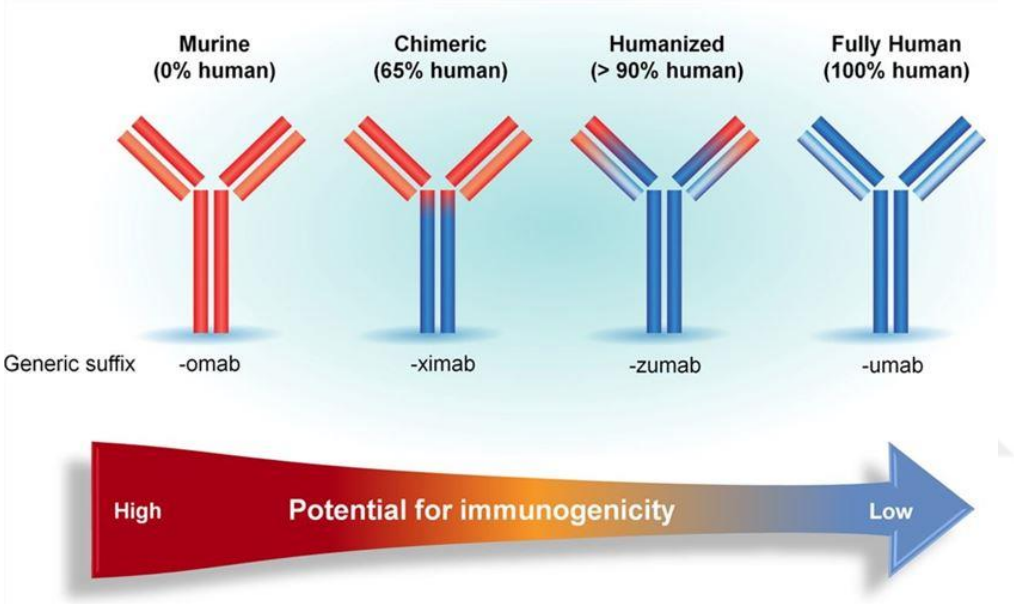


**Figure 1.6 :** Structure of mAb and modifications[24].

Monoclonal antibodies obtained by biotechnological processes can be divided into four main types as murine, chimeric, humanized and fully human antibodies as can be seen in Figure 1.6. Monoclonal antibodies can be modified by genetic engineering to decrease their immunogenic effects to humans in order to be used as therapeutic agents. Therefore, replacing the foreign sequence (i.e. murine originated) in an antibody with sequences originated from human immunoglobulins is possible, and in this way, function loss is prevented. Murine antibodies are directly produced in mouse hybridomas so both chain types are of mouse origin. Chimeric antibodies are synthesized by integrating the antigen-binding variable domains of a mouse mAb to human constant domains. On the other hand, to produce humanized antibodies, the antigen-binding loops which are known as complementarity-determining regions

(CDRs) from a mouse mAb are inserted into human immunoglobins. Humanized antibodies contain fewer foreign sequences than chimeric ones. Therefore, they are assumed to be the less immunogenic ones for humans. Furthermore, humanized antibodies are primarily produced in wild type mice with a native genome including the mouse immunoglobulin locus. On the other hand, fully human antibodies can be produced in genetically engineered transgenic mice with the human immunoglobulin locus [25]. Besides foreign sequences, other factors cause immunogenicity of antibodies such as the method and oftenness of administration, application dose, patients' immune status and disease, the specificity of the antibody to antigens and formation type of immune complex with antigen [26].

#### 1.2.2.2 Monoclonal antibodies in cancer therapy

Antibodies have main roles in the immune system such as the identification of foreign antigens and the warning of the immune system to start the response. The recent emerging technologies in the monoclonal antibody field uses this property to promote antibodies against target antigens existed on the surfaces of tumors and use them in tumor treatment [22].

mAb therapy has been proved to be useful for many widespread diseases such as cancer, autoimmune diseases, and neurological disorders [27]. Even though tumor cells are proliferating at high rates, they are highly abnormal and display several atypical antigens when it is compared to their normal conterparts, but for different reasons they are usually not specifically targeted by the immune system. Utilization of mAbs to flag these unusual tumor cells in the body help to trigger the immune cells towards them [28].

There are several effector functions of antibodies such as modulating cancer signaling pathways by binding to the cancer cell, directing immune cells, or proteins to attack the abnormal cell by flagging them (Figure 1.7). The main function of antibodies is directly inhibiting proliferation of tumor cells by inhibiting key signaling pathways related to cell growth or directly inducing cell apoptosis. Starting antibody-dependent cell mediated cytotoxicity (ADCC) and complement-dependent cytotoxicity (CDC) are other mechanisms for targeting and killing tumor cells [29]. For example, human antibodies such as IgG1 and IgG3 have potential for destroying of tumor cells directly by ADCC or CDC. In the ADCC method, binding of an antibody to a tumor cell

initiates the interaction between the Fc region of antibody and Fc receptors that have found on immune effector cells such as macrophages, neutrophils, and natural killer cells, and thus immune effector cells kill the tumor cells. Moreover, antibodies can direct immune cells like T cells to tumor cells. Finally, cytotoxins such as bacterial toxins, immunotoxins or small toxic molecules like antibody drug conjugates can be directed to kill tumor cells with the help of antibodies [30].

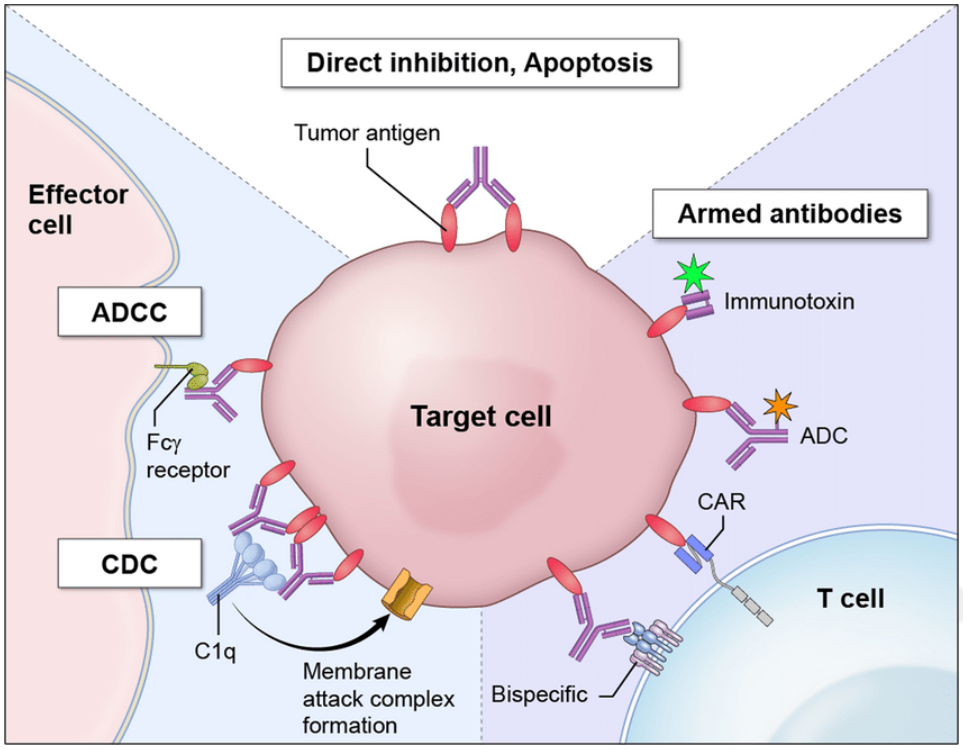


**Figure 1.7 :** Antibody-based cancer therapy mechanisms [30].

The first monoclonal antibody that approved for therapeutic use is Rituximab [31] which shows its activity by selective cellular toxicity. There are several mechanisms to trigger its toxicity. For example, binding of Rituximab to a specific antigen on the abnormal cell can cause to cell lysis or ADCC, CDC, or inhibition of signal transduction like inhibition of dimerization, e.g. binding of Rituximab inhibits the dimerization of a receptor by binding and blocking the receptor with a monoclonal antibody (Figure 1.8 A) [32]. Binding of rituximab to CD20, which is a transmembrane protein present on the cell membranes of all B cells [31], can lead malignant B cells to apoptosis. Moreover, tumorigenic signaling can be inhibited by antibodies (Figure 1.8 B). For example, Cetuximab binds to the epidermal growth factor receptor used in the treatment of colorectal cancer [33]. When the cetuximab binds to the epithelial growth

factor receptor (EGFR), it inhibits the interaction between EGF and EGFR, therefore growth arrest is induced [32].

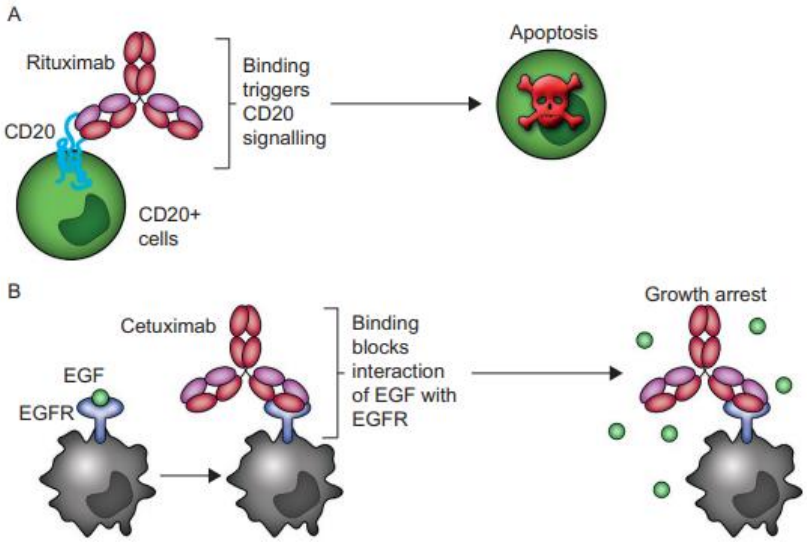


**Figure 1.8 :** Antibody-target antigen signaling modulation. (A) Binding of monoclonal antibody rituximab to CD20 recetors for initiating cell apoptosis. (B) Binding of cetuximab to EGFR [32].

### 1.2.2.3 HER2 targetting mAbs for cancer therapy

HER2 is a human epidermal growth factor receptor, also known as EGFR2 [34], which is a member of the transmembrane tyrosine kinase receptors family[35]. It is encoded by the neu proto-oncogene, and it has been related with augmented tumor aggressiveness [36]. This receptor is highly expressed in several tumors types, thereby it is a good target for mAb related tumor therapies in many solid tumors like breast cancer [37], ovarian cancer, non-small cell lung cancer, prostate cancer and so on [38]. For example, in invasive epithelial ovarian cancer, the percentage of overexpressed HER2 positive cases have differed from 1.8% to 76%[36]. Overexpressed HER2 representation can be seen in Figure 1.9. Over-expression and extracellular accessibility of this oncogene receptor offers great potential for advancement in drug treatment therapies, the development, and improvement of particular aggressive kinds of breast cancer [39-41].

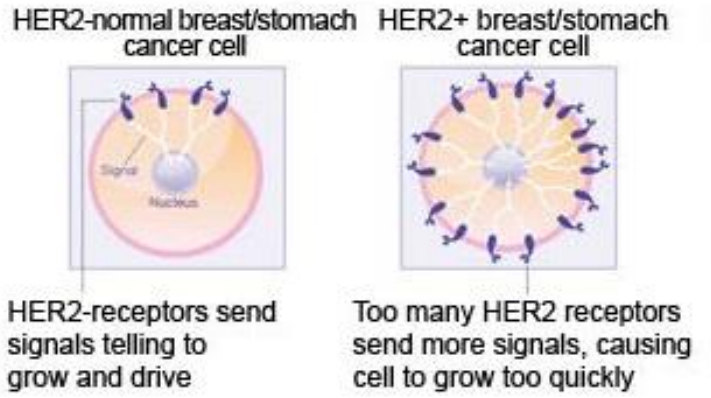


**Figure 1.9 :** Overexpressed HER2 receptors on tumor cells[39].

### 1.3 Characterization techniques of biotechnological drugs

Biotechnological drugs can work efficiently in many illnesses that previously believed to be irremediable. There are already many biological medicines that are authorized and commercially available with expired patents. In that case, a biotechnological medicine similar to already existing ones can be produced [42]. These drugs are commonly known in Europe as 'biosimilar' and, in the USA, known as 'follow-on biologic' [43]. These terms come from the challenges encountered in every stages of biotechnological drug production process when compared with chemical drugs [11].

The critical quality properties of mAb-based drugs such as protein structure, post-translational modifications in the protein, the binding activity, and biomolecular and cellular function levels are required to be analyzed and profiled in detail during both development stages and comparing two versions of biopharmaceutical agent [11, 44]. Therefore, each step from the protein expression to the final product in the mAb production processes should be robustly controlled to assure quality and consistency (Figure 1.10).

The functional assessment (Figure 1.10) is one of the crucial stages that includes biological activity assays that must be established for each biopharmaceutical final product before the product is ready for the market to be used by patients. To confirm the biological activity of the biotechnological drug, cell-based potency assay is the most common technique that allows the evaluation of the biological activity quantitatively. Biological activity is the most crucial property that needs to be strickly controlled by potency testing [45]. Several procedures originated from various

techniques such as animal-based, ligand and receptor interaction-based, cell culture-based, or other biochemical (enzymatic) assays can be used for test the potency of the product depending on the action mechanism of the product [46].

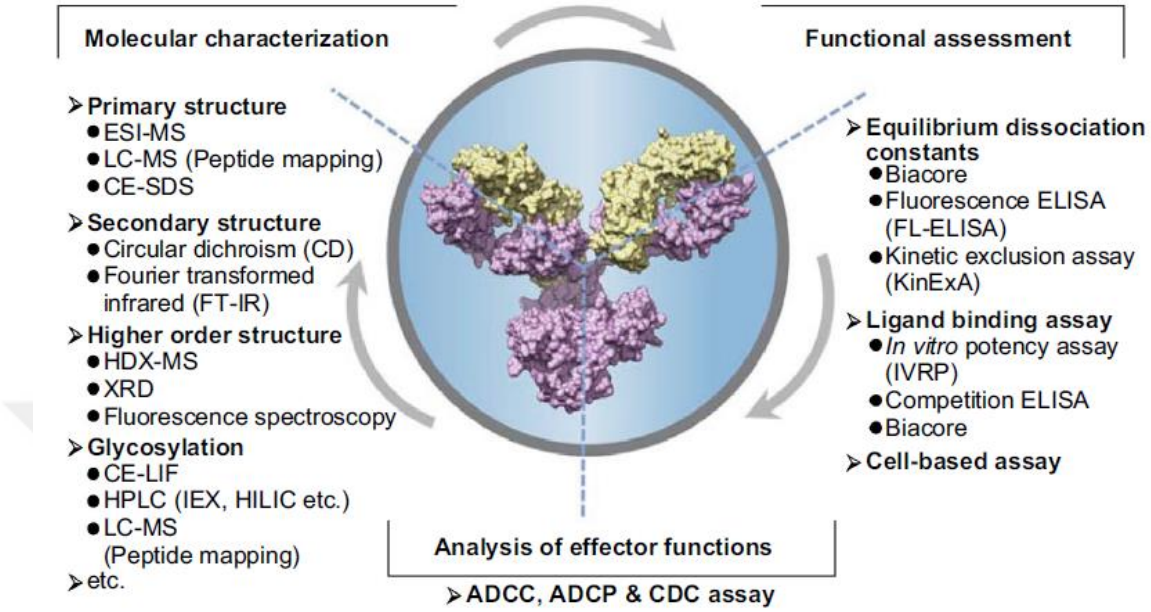


**Figure 1.10 :** Methods for analysis of the molecular structure and function assessment of mAbs. The example mAb is monoclonal antibody is figurative to IgG1[44].

### 1.3.1 Ligand-binding potency assays

To evaluate the binding potency of mAb to its target for ligand binding assay, a stable and soluble target antigen is required. There are several methods to perform in vivo ligand binding assays, but ELISA (Enzyme-Linked ImmunoSorbent Assay) and SPR (surface plasmon resonance) are the most common ones used for commercial tests.

#### 1.3.1.1 Enzyme-linked immunosorbent assay (ELISA)

Enzyme-linked immunosorbent assay (ELISA) is an in vivo assay method developed for detecting and quantifying biological molecules such as peptides, proteins, antibodies, and hormones [47]. In this technique, the antigen immobilized on a solid surface is required. In the assay, the antibody binds to its target antigen, and after the binding, an enzyme-linked secondary antibody is used to obtain detectable signal. For this, the activity of the conjugated enzyme is evaluated by incubation with a substrate which produces a measurable signal which is mainly a color change [48]. The most important fact in the detection strategy is the specificity levels of antibody-antigen interaction. In ELISA assays, EC50 value which is half-maximal effective

concentration shows effective concentration of analyzed target molecule such as drug or antibody and it is useful to compare different batches [49].

There are four ways to evaluate antibody binding with ELISA (Figure 1.11). Format A is also called as non-competitive sandwich assay in which the test antibody is introduced to an antigen-coated 96-well plate, followed by a washing step. The bound antibodies are then detected with the help of labeled secondary antibody by measuring the optical density (OD) or fluorescence. The optical density of the reaction products that occurred in reaction wells is distinctively relative to the analyte amount that measured [48]. The binding ability of mAb can be measured and demonstrated as a binding curve graph with serial dilution method. To interpret the results, the EC50 value of the standard molecules is compared with the test mAb, and thereby the higher the EC50 value means the greater activity of the binding [49].

In the further steps of drug development, competitive ELISA is the preferred method to analyze purified molecules, because it enables the more definite information about the candidate molecules [44]. There are three different methods of competitive ELISA to detect mAb's binding activity. The first format (Format B in Figure 1.11) is including specific antigens and serially diluted test mAbs. In this method, these two components are premixed with a labeled standard of constant concentration. When the specific antigens coated on the surface are treated with this test mAb and labeled standard mixture, a competition between these two is expected. On the other hand, in the second type of competitive ELISA method (Format C in Figure 1.11) a standard mAb is used as a coating agent. To see binding ability, first, a serially diluted test mAb and a labeled antigen are mixed by equal amounts than introduced to standard mAb coated wells. For final assessments, EC50 values were determined. In the final format, if there is an antigen-specific ligand, ligand blocking assay-based competitive ELISA can be designed. The ligand blocking assay (Format D in Figure 1.11), which is similar to Format B, but in this case, the labeled antibody is substituted with a labeled ligand binding molecule [44].

In summary, both non-competitive (Format A) and competitive ELISA (Format B to D) could be designed efficiently and simply. Moreover, competitive ELISA provides analyzing the binding activities of therapeutic antibodies quantitatively, thereby it is preferred for further steps of drug development studies. [44].

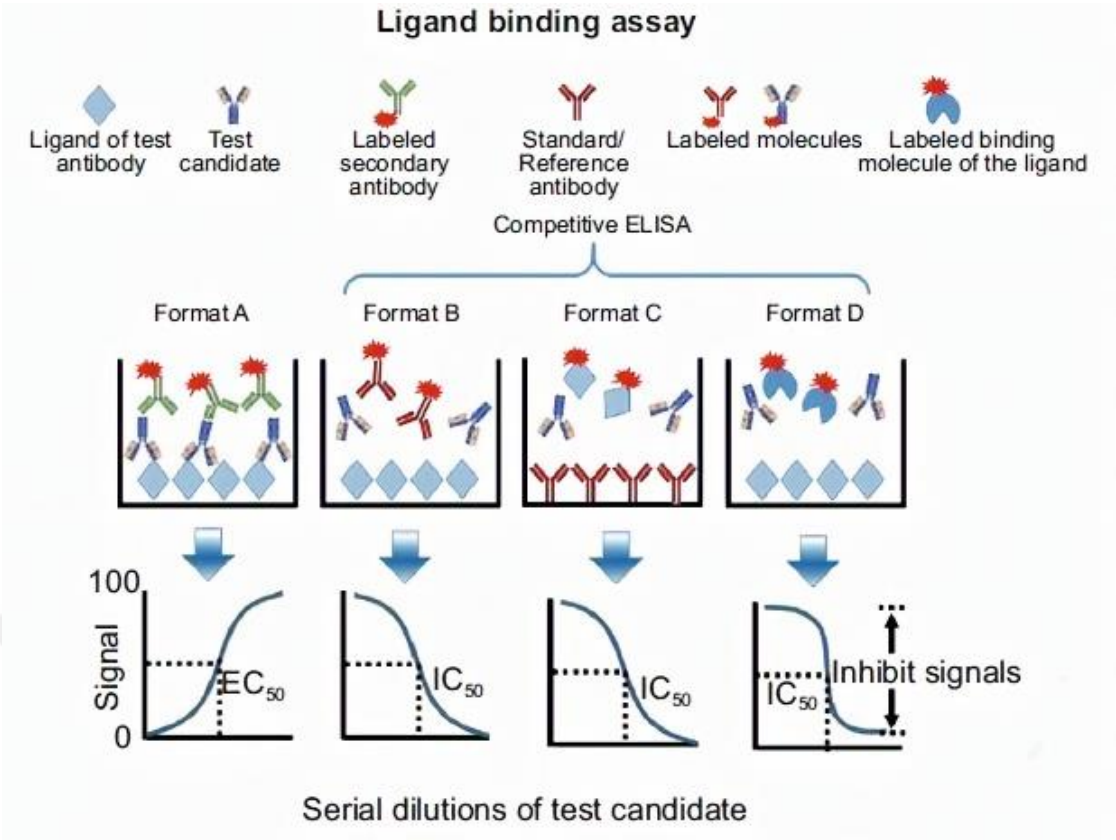


**Figure 1.11 :** Schematic diagram of ligand-binding ELISA assays. Format A; direct analyzing binding activity method. Formats B and C are competitive ELISA examples; Format D is a ligand-blocking assay as a competitive format like format B and C [44].

### 1.3.1.2 Surface plasmon resonance (SPR)

The surface plasmon resonance (SPR) technique provides the real-time monitoring and detection of binding activities of biological molecules without any need for labeling [50]. In SPR analysis, the target molecule (e.g. receptor) or cell is coated to the biosensor surface, and the drug candidate (e.g. mAb) is passed through the sensor surface with a continuous flow across the microfluidic system (Figure 1.12). There are several commercialized SPR devices in the market as a leading technology for direct, real-time, label-free analyzing of the biomolecular binding events [51]. The signal is measured as Response Units (RU) and it is relative to the mass change on the surface [52]. SPR experiments can be designed the same as ELISA assays as seen in Figure 1.11. Unlike ELISA setups in which binding event is followed under no-flow conditions in a plate-well, in the SPR technique, the target molecule (mAb) must be captured while introduced by flow-through system [3].

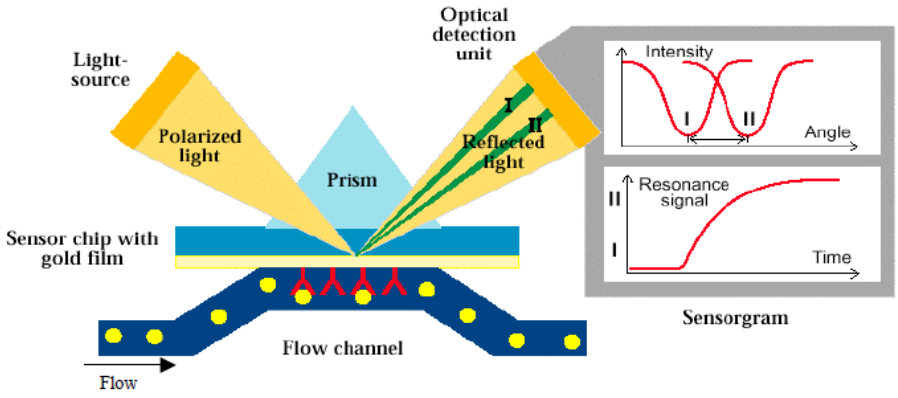


**Figure 1.12 :** Biacore SPR technology. Red Y-shapes indicates ligands and yellow spheres are target molecules (analytes) [3].

In SPR sensors, an interface with thin metallic surface (usually gold layer of 50 nm) and dielectric solution (e.g. aqueous solution) are used. When the light goes across from a higher refractive indexed area (prizm in Figure 1.12) with a specific angle, no light is refracted through the interface and at this moment Total Internal Reflection (TIR) is seen [53]. When the TIR occurs, the evanescent wave, which is an electromagnetic field component, permeates a short distance inside the buffer [54] i.e. roughly 300 nm in BiacoreTM sensors, but this area relies on the SPR system [3]. The incoming light photons react with the gold metal film's free-electron cloud at a certain angle which is known as the SPR-angle. This event induces a decrease in the reflected light at the specific SPR-angle. The SPR angle relies on the refractive index of the buffer side and only sensitive to changes in the evanescent wave range [55]. Therefore, when the biomolecules bind to the sensor surface, this range will be occupied with the molecule and this will induce a change in the SPR-angle relative to the mass increase. Consequently, this system enables the analysis of binding activities of biomolecules to the sensor surface in real-time, continuously, label-free. Finally, the change in the angle is expressed as RU that 1 RU corresponds to a change of 0.0001° or roughly 1 picogram protein [3].

#### 1.3.1.3 Cell-based potency analysis

Cell-based assays are frequently preferred assay types for the determination of potency. They directly measure the physiological response of cells triggered by the product binding, which is only based on interactions between the product and its specific target. Cell-based potency assays can be designed depending on the acting

mechanisms of the products, thereby many different forms are available [44, 56]. The most popular examples of cell-based assays used for characterizing the monoclonal antibodies are apoptosis, proliferation, and cytotoxicity assays. These assays are used to measure triggering, or inhibition of functionally necessary signal molecules such as enzymes, cytokines, cyclic adenosine monophosphates (cAMPs) [45].

Although the ligand-binding assays (ELISA, SPR) can be carried out easily with high precision and accuracy, they may not reflect the true biological potency of the product. When the ligand binds to its target, it can cause several downstream events [44, 56], thereby only measuring the binding activity with binding assays might not give the whole picture [45]. For instance, mAbs with several targets usually trigger an early response through signaling pathways or they can cause a late response as proliferation, or inducing signal molecules such as cytokines, cAMPs. To perform a potency assay on cell level, a downstream marker which is usually inhibited when the interaction occurred with the mAb should be determined. To perform quantitative or qualitative analysis, the biological activity levels are compared with the corresponding control assays.

The therapeutic mAbs commonly target cell-surface receptors of abnormal cells or cytokines. Figure 1.13 shows a cell-based assay example for the mAbs targetting cytokines. To understand the action mechanism of mAbs, a specific cell line is needed (Figure 1.13). For example, Avastin (mAb used in the treatment of metastatic colorectal cancer) is intended to specifically bind to vascular endothelial growth factor (VEGF) to inhibit the interaction between VEGF and VEGF receptors (VEGFRs) on the surface of endothelial cells, and therefore it can inhibit the angiogenic activity of VEGF's [57-59].

Briefly, cell-based potency assays are not only helpful to analyze the biological activity of antibodies but also useful for understanding the effect of chemical modifications that can be occurred on the target mAbs during the production process [44]. These effects can not be obtained with ligand binding assays [44, 60]. Therefore, cell-based assays should be fundamentally preferred assays for final product characterization or at early development stages [44, 45].

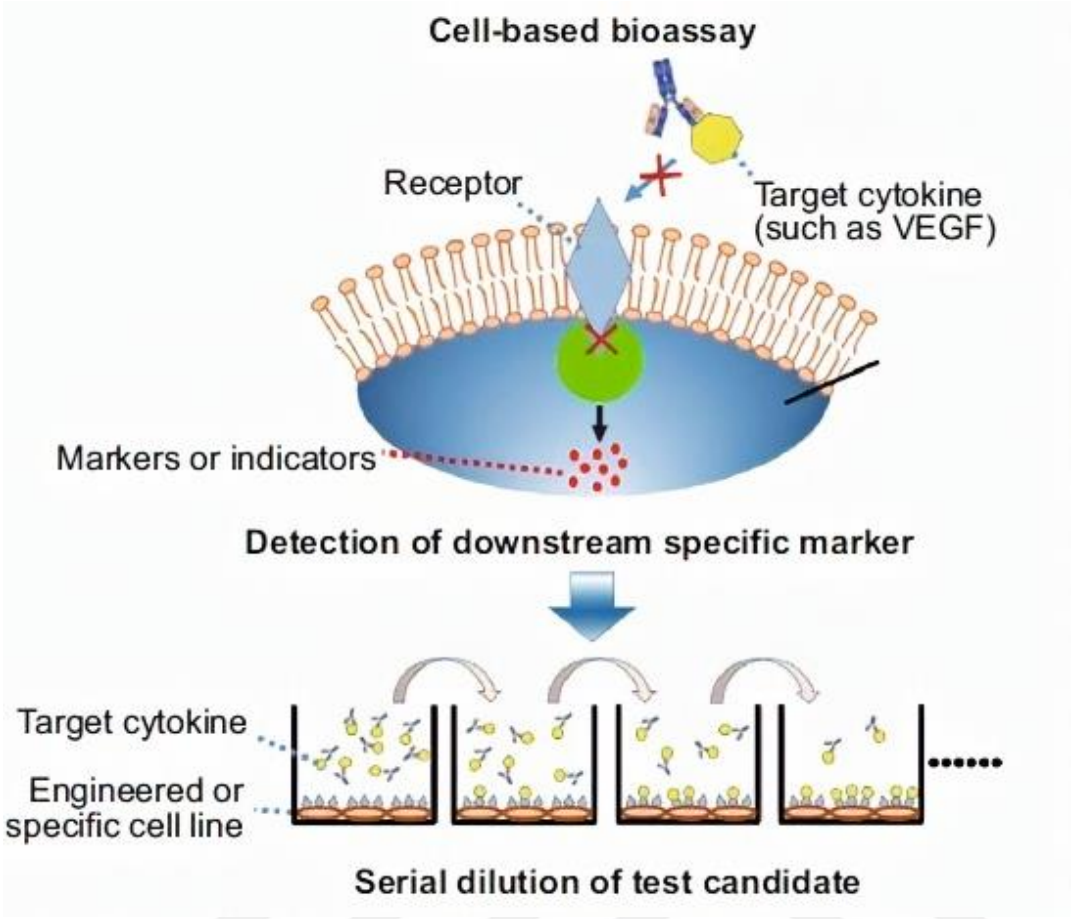


**Figure 1.13 :** Schematic diagram of cell-based potency assay [44].

## 1.4 QCM-D for Characterization Studies

### 1.4.1 QCM-D

The QCM-D technique is broadly used to investigate interactions between molecules with different characteristics and surfaces thanks to its unique features that enable both determinations of adsorbed mass change on the surface and characterization of the viscoelastic properties of the adsorbed layer [61]. The working principle of QCM-D is depending on the piezoelectric nature of quartz crystal (Figure 1.14a). The QCM-D sensor is composed of a quartz crystal that is inserted between two electrodes (Figure 1.14b). AC electric field is applied to obtain a shear oscillatory movement of the quartz (Figure 1.14c) [62]. By implementing an adequate alternating voltage at a frequency that similar to the resonant frequency (f0) of the quartz, a mechanical oscillation is obtained [63]. In the QCM-D system, the mass change is indicated with a change in the frequency values (Δf) and viscoelastic properties are reflected with a change in the dissipation values (ΔD).

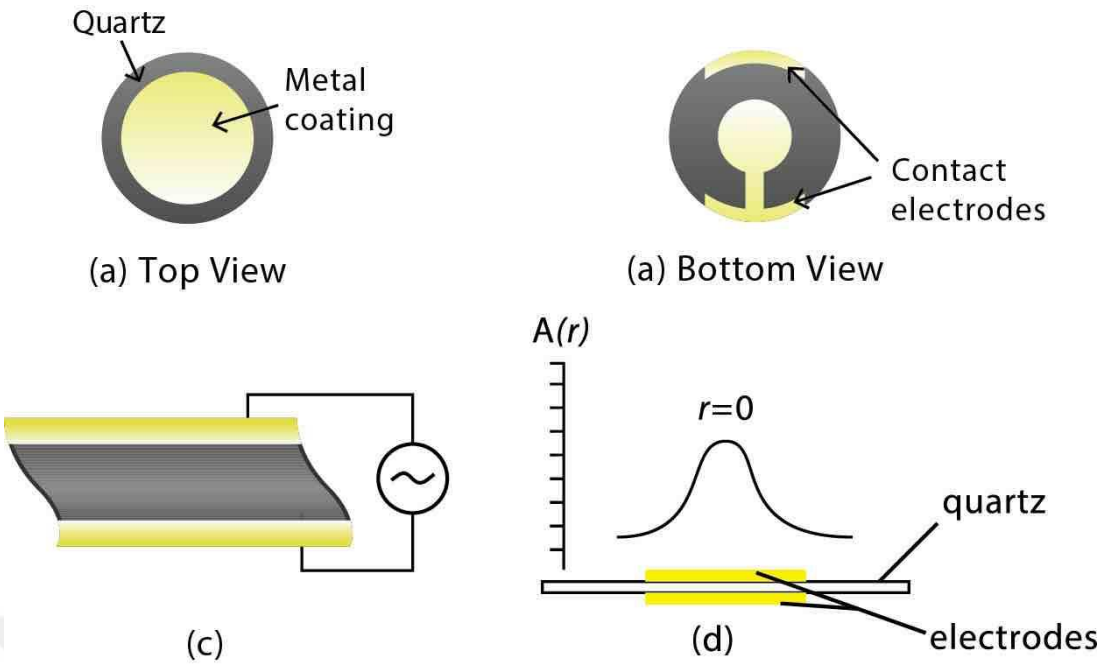


**Figure 1.14 :** Overview of quartz crystal with electrodes in which grey indicates crystal and yellow indicate electrodes. (a) topside view of the crystal (b) bottom side view of crystal. (c) A schematic example of AT cut crystal with the application of AC voltage. (d) A schematic example of vibration amplitude of (A(r)) which differ from the center of the sensor with the distance (r)[64].

The resonant frequency of this oscillating crystal is responsive to mass changes at nanogram-scales [65]. According to Sauerbrey's basic theory (developed in 1959) [66], the change in the frequency (Δf) of a quartz crystal resonator is a direct function of the adsorbed mass (Δm) as can be seen in Equation 1.1. In this equation, Δf refers to resonant frequency, Δm refers to the mass placed at per unit crystal surface area, and C is the mass sensitivity constant of the device. When the crystal is at 5-MHz, C value equals to 17.7 ng/Hz·cm2 [67].

$$\Delta m = C\Delta f \qquad \text{Eq. 1.1 [66]}$$

This equation, known as the Sauerbrey equation, is accurate when the mass of the quartz crystal is bigger than the mass deposited on its surface and in that case the mass is assumed to be equally dispersed. However, crystal sensitivity to deposited mass is not the same throughout the surface, but follows Gaussian distribution also known as a normal distribution [68] which displays a maximum at the center of the sensor and reducing towards the edges (Figure 1.14d) [69]. This dissimilar mass sensitivity of the quartz surface area is another limitation of the Sauerbrey equation. Consequently, this equation is suitable only in limited situations such as rigidly adsorbed, equally distributed, and limited mass amounts over the active area of the crystal.

Another factor to be considered is the viscosity and elastic properties of the samples interacting with the surface. Viscoelestic samples causes to dampening of the resonator, thereby they do not fit the Sauerbrey relation assumption and this situation led researchers to find new methods to re-explain the signals and analyzing mass depositions with frictional dissipative losses because of their viscoelastic character [70] [71]. One of the methods to interpret the dissipative losses originated from viscoelastic materials is to monitor the decomposition of a crystal's oscillation. When the liquid coupled material adsorbed to the sensor surface, oscillating quartz crystals sense the layer as a viscoelastic or hydrogel. If the adsorbed layer is viscoelastic, it will not match completely to the crystal oscillation and there will be a dampening in the oscillation of the crystal. This dampening will result in a reduction in the crystal quality factor (Q). The Q factor holds all the data about the resonation properties of quartz crystal in the surrounding media. This means that the effects of adsorbed layers properties of on the quartz crystal is indicated with the Q factor [63, 69, 72]. The damping also can be called dissipation (D), which is the inverse of Q, gives information about the viscoelasticity of the adsorbed layers. D can be explained as the energy lost ratio, during the one oscillation cycle to the total energy kept in the oscillator (Equation 1.2) [63].

$$D = \frac{Elost}{2\pi Estored} \qquad \text{Eq. 1.2 [63]}$$

Thus, the viscoelasticity or rigidity of the adsorbed layers can be determined by the second generation of QCM machines called as QCM-D [73]. More definitively, rigid materials match easily with the oscillating quartz, therefore when the applied voltage is stopped, the decay of oscillation takes longer which means the decay curve will be longer as can be seen in Figure 1.15b while if the adsorbed mass is viscoelastic molecules like cells, proteins, etc., the coupling of these materials will not be fitted to quartz oscillation and resulted in fast decay and a shorter decay curve (Figure 1.15c).

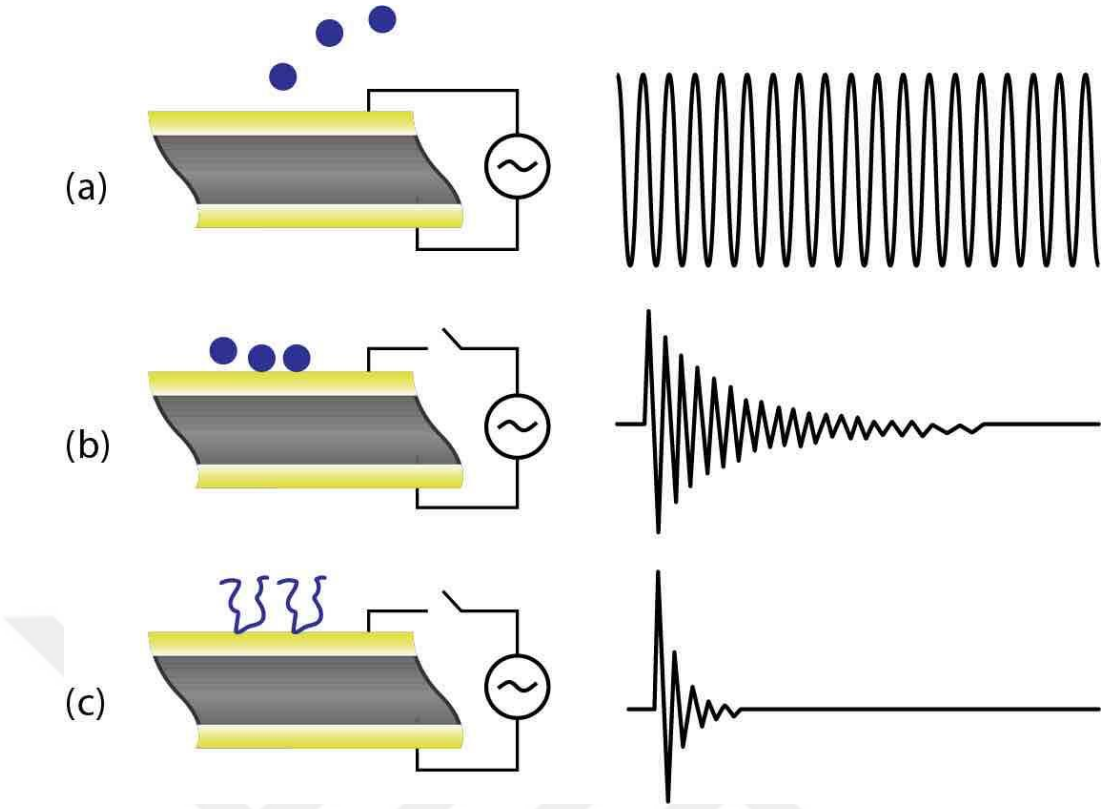


**Figure 1.15 :** QCM-D principle. (a) the oscillation frequency before mass adsorption. (b) Rigid mass coupling to sensor surface. (c) Viscoelastic mass coupling to sensor surface [64].

Another advantage of using QCM-D is the ability to use different overtones to perform depth-related analysis. The spread of acoustic wave across the sensor surface is afflicted by the fluid changes that entrapped in the analyte. The sensing depth is limited to an area extending to ~250 nm at the fundamental frequency of 5 MHz [70]. But, adjusting the sensing depth can be done by altering the frequency overtones, i.e. when the overtones (fn) is increased, the sensing depth decreases. Parameters like thickness, density, mass, or viscoelasticity can be modeled easily by recording both dissipation and frequency at several harmonics such as n= 3, 5, 7, 9, 13 [74]. Thus, the different overtones give information about the homogeneity or heterogenity of the adsorbed layers [70].

### 1.4.2 Cell interaction studies in QCM-D

QCM can be used in many bioanalytical applications such as characterization of the affinity between receptors and their soluble ligands, cross-linking studies of proteins, DNA hybridization, or interactions between DNA and drugs likewise the adhesion and spreading of cells and drug treatments studies on cells [75, 76].

Lately, QCM-D based whole-cell studies have been started to be attractive to researchers. The QCM enables specifically monitoring the cell attachment and spreading on the sensor surface of the quartz crystal [70, 77], and supply the evaluation of the kinetics of the process in real time.

Cell adhesion to substrate requires many synchronized molecular interactions which are both related with the internal and external elements of the cell. Cell adhesion process is necessary for all cells for survival, differentiation, and movement. Mainly three stages occur during the process; first loose cell attachment occurs, then cells flatten, and then they start to spread their membrane over the surface as can be seen in Figure 1.16. At the same time, adhesion complexes are formed with intracellular actin filaments, also known as stress fibers, via integrins to be attached to the extracellular matrix (ECM) [78].

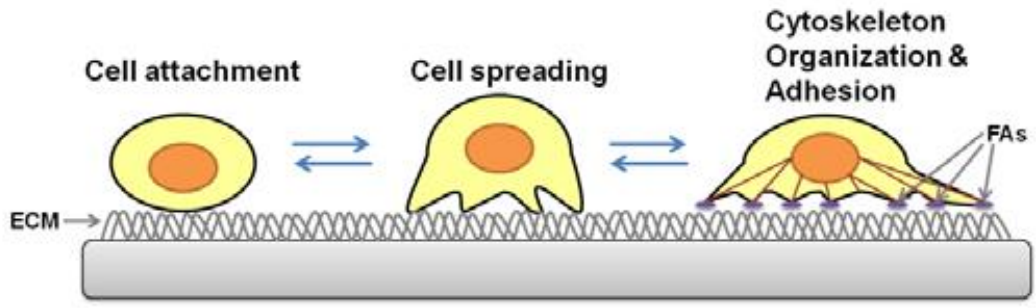


**Figure 1.16 :** The process of cell adhesion [65].

Actin filaments are one of the cytoskeleton components located near the plasma membrane in animal cells (Figure 1.17), but their organization and dispersion rely on the cellular type. Actin filaments display several functions in the cells during cell division, phagocytosis, endocytosis, or communication of organelles [79]. Mechanical support for maintaining or altering the cellular shape and cell attachment forces to surfaces through focal adhesions is provided by actin filaments in the animal cells [80]. Anchoring of the cells firmly to the substrate surface is provided with focal adhesions (FAs) which are the results of adhesion complexes. There are critical roles of focal adhesions in the cells such as migration regulation, proliferation, and cell differentiation [81]. Therefore, QCM based cell assays can be used to understand these critical events as a unique assay that provides information about the cell behavior.

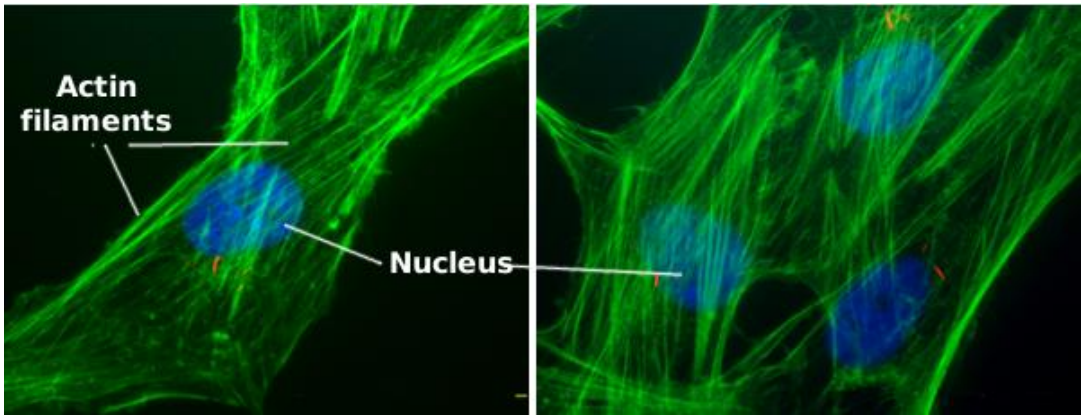


**Figure 1.17 :** Actin filaments stained with green color in cultured cells. Blue indicates the nuclei of the cells [79].

### 1.4.3 Drug binding studies in QCM-D

Cell-based assays are important in the development of drugs and diagnostics as explained in Section 1.3.1.3. Early drug development assays are grounded on in vitro assays, but cell-based assays provide extensive knowledge about the biological effects of the drugs [82]. Conventional drug binding studies depend on the evaluation of the interactions between purified cell membrane receptors and antibodies [75]. For example; ELISA can take long times, costly, and sometimes not sensitive enough [83]. In addition, some studies show that labeling of cells or antibodies can affect the quality of interactions and cause to an increase in non-specific binding [84], which underlines the primary advantage of the QCM-D technique as a label-free analytical tool [75].

QCM-D can provide a real-time cell-based assay for studying drug binding [75, 85] and unlike the other biosensors that use purified and immobilized target molecules, it enables to work directly with cells and receptors in their native environment [75]. To study binding events when the targets are in their natural environment like cell membrane or live cells give more reliable information so cell-based biosensors are rising tools [75, 76]. The existence of other cell membrane components in whole cells can also influence the binding features so binding to isolated receptors may not give the correct knowledge on physiological interaction [86].

Elmlund *et al*. [75] studied the binding of a mAb to the HER2 receptor on SKOV3 epithelial cancer cells by using quartz crystal microbalance (Figure 1.18). In their study, the SKOV3 cell line was fixed to the sensor surface. After fixation, mAb was passed over the surface to bind the HER2 receptor which is found on the cell membrane. This study allows them to measure the direct interaction with intact cellular

receptors and provided quantitative binding data. In this study, although the antibody-HER2 interaction studies offer a novel aspect on the affinity in a more natural environment, it does not provide information about the binding effects of mAbs on alive cells. It shows only changes in frequency due to mass change because of mAb binding and but cellular activities cannot be measured since the cells are fixed. On the other hand, in our study, we used alive cells to analyse binding activities of HER2 targeted mAbs. We observed the changes in cell-surface interface as a result of mAb binding in real time, not the mass increase that occurred because of mAb binding.

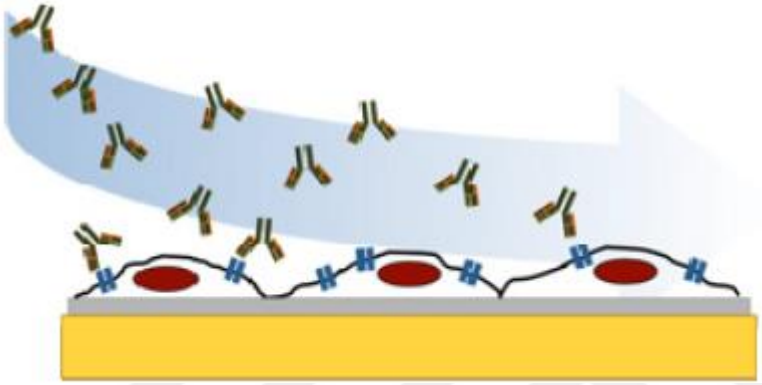

**Figure 1.18 :** Simplified illustration of monoclonal antibody binding to HER2 receptors. Green and yellow colors with Y-shapes molecules are monoclonal antibodies, blue is HER2 receptor on SKOV3 cells that fixed to QCM sensor [75]

# 2. MATERIALS & METHODS

## 2.1 Materials & Equipments

The laboratory materials and devices used in the experiments were listed in Appendix A and the chemicals used in the experiments were listed in Appendix B.

## 2.2 Methods

### 2.2.1 SKOV3 cell culture

SKOV3 (human ovary adenocarcinoma, ATCC HTB-77) cancerous cell lines which is kindly provided by Arven Pharmacuticals were incubated with standard subculturing in 5% CO2/95% air atmosphere at 37°C by a humidified incubator. 75 $cm^2$ cell culture flasks are used for incubation and growth of cells in Dulbecco's modified Eagle culture medium (DMEM) containing high glucose (5 g/L), sodium pyruvate (3.7 g/L), and 1% (v/v) of penicillin-streptomycin and completed with 10% (v/v) fetal bovine serum. The cells were usually harvested at 80% confluency and detached from the flask by trypsinization with 0.20% trypsin–ethylenediaminetetraacetic acid (EDTA) solution at 37°C for 5 min. After the trypsinization step, enough serum-completed culture medium was added to the flask for inactivation of trypsin and the cells were centrifuged at 1000 rpm for 5 min. The pellets were suspended in a serum-completed medium and a viable cell number was determined on hemocytometer with trypan blue exclusion under the microscopy. The principle of the Trypan Blue dye exclusion test is built on that live cells possess undamaged cell membranes that exclude specific dyes such as trypan blue, whereas dead cells can not. To determine the number of viable cells, both equal volume of trypan blue dye and the cell suspension was mixed by using a pipette to get a 1 to 2 dilution (100 µL of cells to 100 µL of trypan blue). Then, the hemacytometer counter with the coverslip previously in place was filled with the cell suspension by placing the pipette tip to the notch. Then all viable cells in each large square in each corner of the hemacytometer (shown

as Figure 2.1) were counted under the light microscope and then viable cell count (live cells per milliliter) were calculated using Equation 3.1.

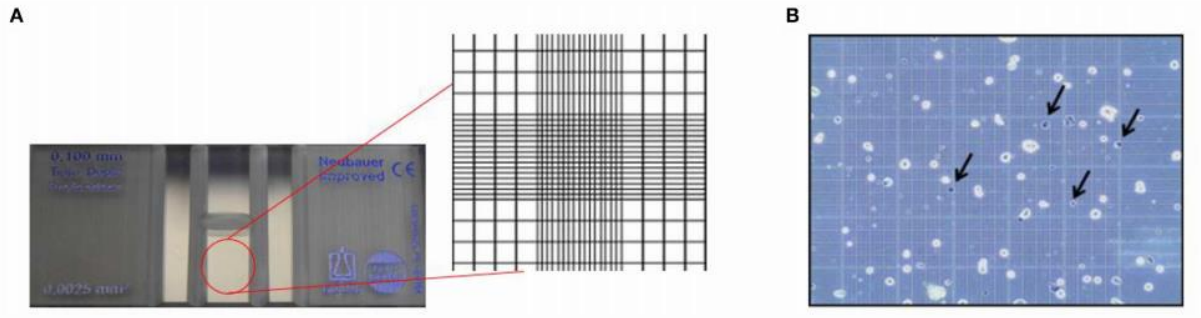


**Figure 2.1:** Cell counting principle in a hemocytometer. (A) Neubauer chamber with counting grid in hemocytometer as zoomed. (B) Trypan blue dye stained cells where the arrows show dead cells[87].

$$Viable\ Cell\ Count = \frac{\#\ Live\ Cells\ Counted}{\#\ large\ corner\ Squares\ counted}\ x\ Dilution\ factor\ x\ 10000 \qquad \text{Eq. 3.1[88]}$$

### 2.2.2 Quartz crystal microbalance with dissipation (QCM-D) measurements

#### 2.2.2.1 Preparation of biosensor surface

AT-cut gold-coated quartz crystals with 5 MHz fundamental frequency and 14 mm diameter were used in QCM-D experiments. Oxidized gold-coated quartz crystal surfaces (hydrophilic) were utilized for all trials. For the obtain hydrophilic surfaces, sensors were exposed to UV-ozone for 15 min. Before cell seeding, sensors incubated for 30 minutes with 70% ethanol in a petri dish to be sterilized and rinsed with 0.1 M phosphate buffer saline (PBS) three times.

#### 2.2.2.2 Preparation of QCM-D

QCM-D experiments were accomplished with a dissipative QCM instrument (Figure 2.2) both with and without a flow-through system. Both the frequency (Δf) and dissipation change (ΔD) values in different overtone frequencies as 15, 25, 35, 45, and 55 MHz harmonics, were acquired but only the third overtone frequency shift (Δf3/3) and dissipation change (ΔD3) results were used to make interpretations. The liquid flow across the measurement cell was kept constant at 100 µL/min via a peristaltic pump. All measurements were applied at 37 °C.

**Figure 2.2 :** The electronic unit and the fully assembled QCM-D device.

QCM-D system, the reaction chamber, and the tubings were cleaned before each experiment with sodium dodecyl sulfate (SDS; 1%), ethanol (70%), and degassed ultrapure water in orderly. After cleaning, the reaction chamber was dried with $N_2$ gas.

Cell seeded sensors were then inserted into the measurement chamber and the all system was assembled as shown in Figure 2.3. Sterilized tweezers were used when replacing the o-ring and the sensor itself as these parts were in straight contact with the cells and drugs during the measurements.

**Figure 2.3 :** The reassembly of the measurement cell.

### 2.2.2.3 Cell seeding on biosensor surfaces

Oxidized gold-coated quartz crystals sensors were incubated with cell suspension in a humidified CO2 incubator (5%) with the serum-supplemented medium. First, the measurement conditions, i.e. initial cell amount and cell incubation time, were optimized. For this, different plate types, namely 6-well, 12-well plate, and petri dishes, were tried and a 12-well plate was chosen since it provides better cell distribution. Different initial cell numbers, 50k, 100k, 250k,

were used to see the effect of cell number on the QCM-D signal. To understand the effect of incubation time on QCM signal, different incubation times such as 15, 20, and 24 hours were tested. When incubation was ended, the medium was kindly removed, and the sensors were gently washed with PBS. After washing with PBS, sensors were replaced to the QCM chamber and the effect of drug presence on adhered cells was observed by following the changes in resonance frequency value (Δf) and energy dissipation value (ΔD).

After each measurement, $H_2O$:$NH_3$(25%):$H_2O_2$(30%) (5:1:1) solution is used to clean the crystal sensors. Sensors were kept for 5 min at 75 °C in this solution to remove the organic residuals from surfaces. Following cleaning, they were treated with UV-Ozone in the UV-Ozone chamber for 15 min. Finally, the sensors were rinsed with ultrapure water, dried under N2 gas, and stored in a desiccator until reuse.

#### 2.2.2.4 Effect of the drug on cell adhesion

Real-time QCM-D experiments were performed in room conditions, not in CO2 supplemented incubator. Therefore, to keep the pH of the media at 7.2–7.6, 25 mM 4-(2-hydroxyethyl)-1-piperazineethanesulfonic acid (HEPES) was added to media as a supplemental buffering system. To prevent contamination of media, 1% (v/v) of the penicillin-streptomycin solution was used to complete the media content. The media which was used in all QCM experiments was a serum-free medium with HEPES buffering.

All the media and drug (HER2 specific monoclonal antibody/HER2-mAb which is kindly provided by Arven Pharmacuticals) solutions were kept in room conditions to be equilibrated thermally at room temperature (22–24 °C). Following the equilibration, mediums were introduced to the measurement cell at a rate of 100 μL/min by a peristaltic pump. After inserting the cell-seeded QCM-D sensors prepared as described in Section 3.2.2.3 into the QCM chamber, the medium was passed across the measurement chamber to record the initial resonant frequency of the crystal sensor and obtain a stable baseline (ca. 25–30 min.) before sending the drug-containing media. After obtaining a stable baseline, the medium containing the HER2-mAb was passed through the measurement chamber until the QCM chamber was filled with the drug solution (~ 10 min.). The pump was then stopped, and real-time signals were recorded while the cells were incubated with HER2-mAb in no flow conditions for at least 1.5 hours. To investigate the time-based effect of drug exposure to the cells and their interaction with the

surface, different incubation times, 1.5, 3, and 6 hours were tried. Besides, cells were exposed to HER2-mAbs at distinct concentrations (40, 80, 120, and 160 µg/mL). Each incubation time experiments were repeated at least two times. Each drug trials with different concentrations were repeated at least three times. For the control experiment, the drug-free medium was pumped into the chamber and changes in signals were recorded to show the specific effect of the mAb binding to the SKOV3 cells.

### 2.2.3 Fluorescence imaging of cell-surface and cell-drug interaction

The fluorescence labeling procedures were conducted for two different purposes. Firstly, cell staining protocol was performed for the investigation of cell morphologies and numbers to determine the best cell density for drug trial experiments. In this experiment, different number of cells (50k, 100k, 250k) were incubated for 24 hours and then fixation and staining protocol were performed. In the second experiment, 50k cells were treated with the 40, 80, 120, 160 µg/mL HER2-mAb under identical conditions at QCM-D experiments. After 1.5 hours of incubation, cells were fixed and stained. Each experiment and each parameter were repeated at least three times.

#### 2.2.3.1 Cell fixation and staining

First, cells were washed with PBS three times and then incubated with 4% (w/v) formaldehyde for 15 min to be fixed. After the second PBS wash, cells were treated with 0.5% Triton® X-100 (v/v) in PBS (15 min) for permeabilization. Excess triton was removed by PBS washing and the cell nuclei were stained with 4′,6-diamidino-2-phenylindole dihydrochloride (DAPI; 100nM) by incubating in PBS for 15 min. Bovine serum albumin (3%) was used as a blocking agent for 1 hour. Then, cells were incubated with Phalloidin CruzFluor™ 488 Conjugate (Excitation/Emission wavelength 493/517 nm) for 20 min at room temperature to stain filamentous actins (F-actin). After the final wash with PBS three times, fluorescence images were captured by using an inverted fluorescence microscope at different spots on each surface. Images of the cells were processed by an image processing software (ImageJ Version 1.51n, National Institutes of Health) to examine the cell spreading and morphology. All staining and imaging processes were performed in the dark.

## 3. RESULTS & DISCUSSION

All experiments with the QCM-D were performed in a serum-free medium to eliminate the interaction effects between surface and serum proteins to observe more clearly the adhesion behavior of cells after drug treatments. On the other hand, cell seeding experiments were conducted with standard subculturing techniques in a humidified incubator with 5% CO2 and 95% air atmosphere at 37°C with serum-supplemented media to ensure the spreading cells[89]. Before QCM-D studies, cell number optimization experiments were performed, and cell distributions were analyzed by cell staining and examined under fluorescence microscope to avoid cell stacking and to determine the most suitable cell amount for drug trials. After optimization of the cell number, the suitability of HEPES buffered serum-free medium in QCM-D experiments was examined by staining and visualization of cell morphologies after 3 hours of incubation. In general, pH 7.2-7.4 values are the most suitable culture environment for many cells [90] and the HEPES buffering range is exactly in pH 6.8-pH 8.2, which is convenient for cell culture[91]. Thanks to HEPES buffer and controlled pH values, and 37°C provided by QCM chamber, no difference was observed in the morphologies of the cells for 3 hours as expected[73, 89]. For drug trials, SKOV3 cancer cells were cultivated in cell culture flasks until 80% of confluence [75], then cell moved to suspension and counted, then specific numbered cells cultivated for 24 h on gold-coated quartz crystal sensors optimized for cell attachment. HER2 targeted antibodies were passed over the sensors to allow the binding of the antibody to its target receptor that is present in the SKOV3 cell membrane. Last of all, cell behavior towards the drug treatments was monitored by QCM-D, and cell morphologies were examined.

## 3.1 Initial Cell Number and Cell Distribution Assays

### 3.1.1 Initial cell number

Different initial cell numbers, 50k, 100k, 250k, were used to see the distribution of cells on gold-coated sensors. After fixation and cell staining, the image of cells was captured under 20x objective (Figure 3.1). As can be seen in Figure 3.1, the spread of cells to the surface and morphology of each cell was distinguishable in the 50k case when compared to the 100k. To be able to observe the response of cells without any diffusion limitation during the QCM-D experiment, all drug trials were conducted on 50k cells.

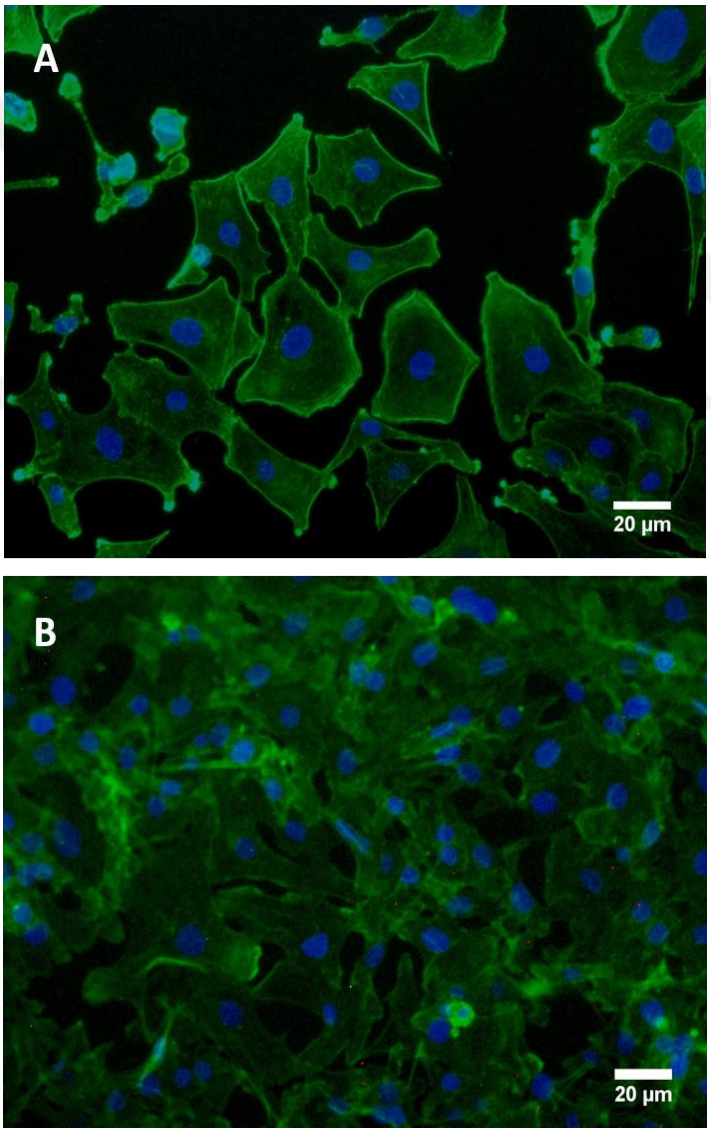


**Figure 3.1 :** The cell number and distribution assays. Fluorescence microscopy images of [A] $0.5x10^5$ and [B] $1x10^5$ cells after 24h, in 10% FBS medium (under 20x objective) (blue: DAPI; green: Phalloidin CruzFluor).

### 3.1.2 Effect of serum on spreaded cell morphologies

Serum-supplemented and serum-free media were used to clarify the effect of serum absence on cell morphology during the experiment, i.e. three hours in which the cells were incubated with the drugs in the QCM chamber. As can be seen in Figure 3.2 and Appendix C, Figure C1, there were no significant differences between cell morphologies in different media conditions.

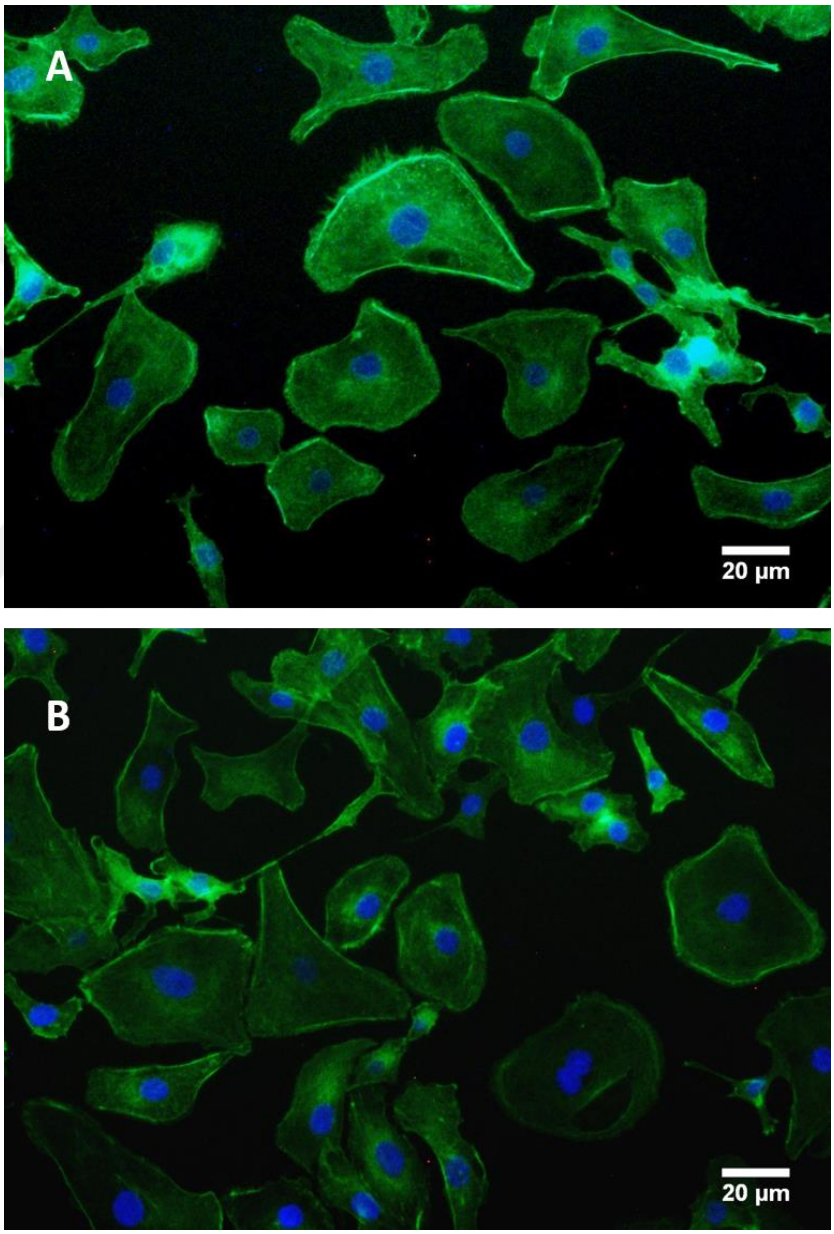


**Figure 3.2 :** Morphology of cells incubated in serum-free [A] and serum-supplemented [B] medium for 1.5 hours the same as drug treatment time. Fluorescence microscopy images of $0.5.10^5$ cells in CO2 independent medium (under 20x) (blue: DAPI; green: Phalloidin CruzFluor)

## 3.2 QCM-D Optimizations

### 3.2.1 Incubation time

Before drug trial experiments, incubation time required for efficient cell spreading was determined. SKOV3 cells had been reported to completely spread to the surface after 24 hours [75, 92]. In our study, experiments were conducted on cell-seeded gold-coated sensors and cells were incubated for 15, 20, and 24 hours after seeding. At the end of the 15, 20, and 24 hours, sensors were placed to measurement cell and serum-free media was introduced at 100 μL/min rate by peristaltic pump. The media was passed through the measurement chamber to record the initial resonant frequency of the crystal sensor and obtain a stable baseline.

As can be seen in Figure 3.3A, frequency changes (Δf) (Figure 3.3A) and dissipation changes (ΔD) (Figure 3.3B) were at similar for both 20 and 24 hours. Furthermore, the stable baseline was obtained within 30 minutes in both 20- and 24-hours incubation. The acoustic ratio, i.e. the dissipation changes per frequency change (in absolute values), $|\Delta D/\Delta f|$ ($GHz^{-1}$), values were also similar for both cases (Figure 3.3C). The acoustic ratio is used to derive information about cell attachment and cell behavior on the surface and considered as unique signatures or fingerprints [70, 85, 89]. The acoustic ratio also gives information about the morphology of the cell, the internal structure of cell, and the dynamic processes that occurred along the cell spreading. According to Kilic's study [70], dissipation value started to remain stable after 9 hours whereas Δf continued to decrease slowly during cell spreading experiments in QCM-D. Although different cell types were used, these findings are consistent with our results. As can be seen in Figure 3.3A, after 20- and 24-hours incubation, Δf values are lower than 15 hours incubation. It can be said that after 20 hours cells completed their spreading to the surface.

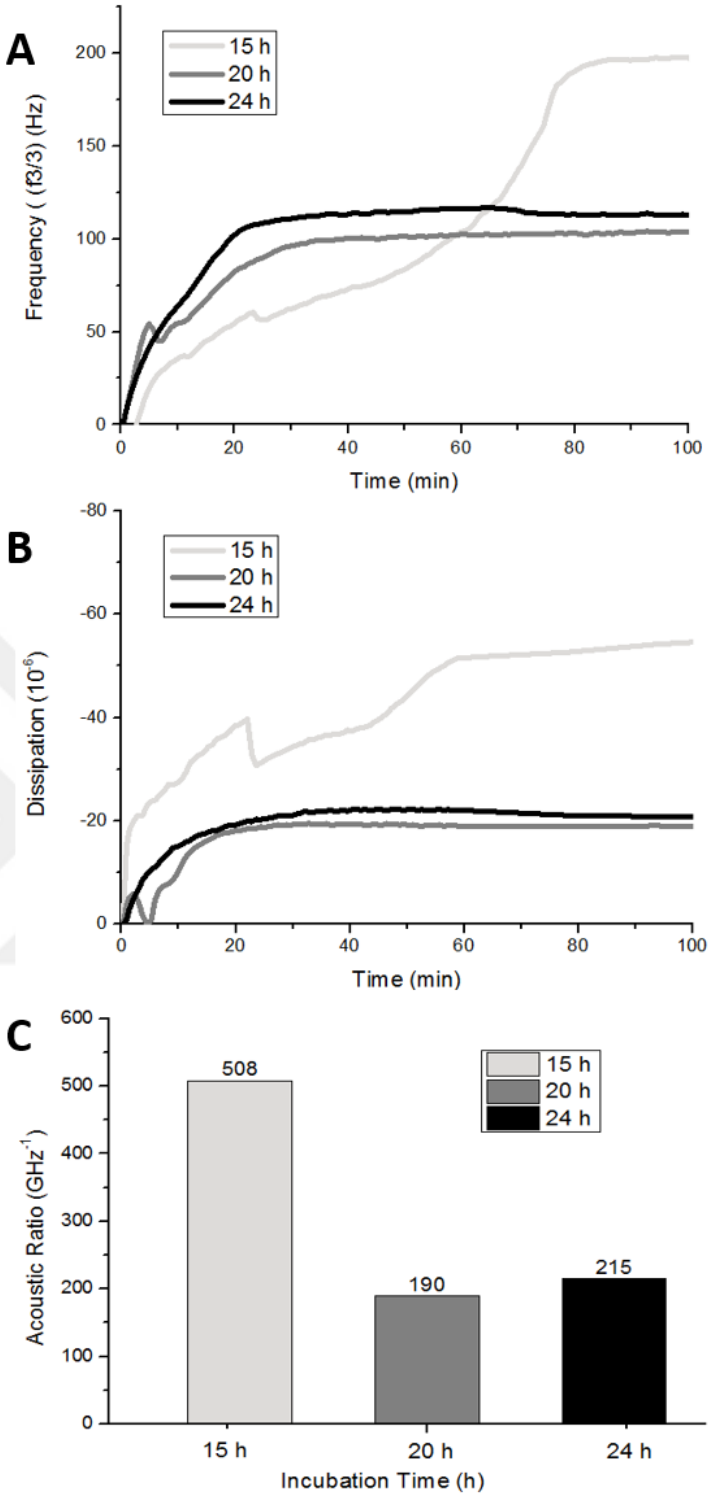


**Figure 3.3 :** QCM-D signals of SKOV-3 cells monitored on treated gold sensor at different hours after seeding. (A) Frequency change (Δf) versus time in 15 (light gray), 20(dark gray), and 24(black) hours after seeding. (B) Dissipation change (Δf) versus time in 15 (light gray), 20(dark gray), and 24(black) hours after seeding. (C) Acoustic ratio versus seeding time in 15 (light gray), 20(dark gray), and 24(black) hours after seeding.

## 3.3 Drug Trials in QCM-D

### 3.3.1 Monitoring cell behavior during trypsin treatment

The presence of alive cells on the sensor surface and the specific, protein-mediated cell interactions [70] was verified by using trypsin solution in the QCM-D measurement cell (Figure 3.4). The first stable baseline was obtained (ca. 30 min) and drug treatment was applied under no-flow condition (ca.75 minutes). The cell culture media and PBS were passed through the measurement cell until a stable baseline was attained in ca. 20 min and 10 min, respectively. The cells were then incubated with Trypsin– EDTA for ca. 10 min. Trypsin breaks down proteins as a proteolytic enzyme, and it can be effectively used to dissociate adherent cells from the surface in which they are being seeded [93]. When the cells treated with Trypsin– EDTA, a decrease in the sensed mass and dramatic change in both $\Delta f$ and $\Delta D$ signals were observed because of the enzymatic splitting of proteins and the complete separation of the cells. Figure 3.4B shows a considerable decrease in $\Delta D$ and a significant increase in $\Delta f$ which can be explained with the detachments of the cells due to the trypsinization process. It can be concluded that there were adhered cells on the surface during the whole experiment steps and alive cells established protein-mediated connections with the surface.

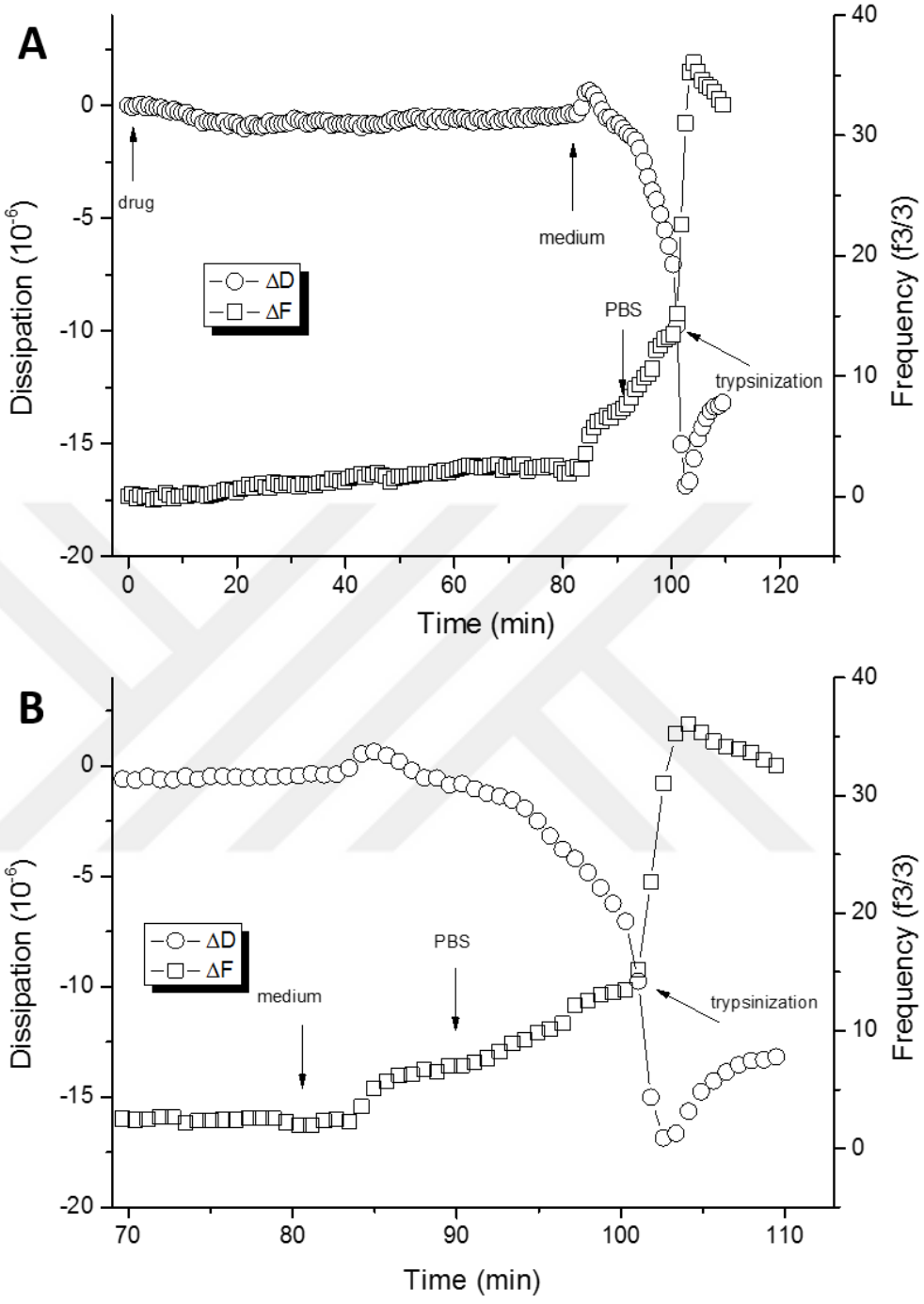


**Figure 3.4 :** QCM-D signals versus time monitored on cell seeded gold sensor. Round shapes indicate Δf, square shapes indicate ΔD. After 80 minutes drug treatment, media was passed through the measurement chamber, then PBS, final treatment was Trysin-EDTA for trypsinization(A). The last 40 minutes of the graph A to show treatments and stable baselines more noticeable (B).

### 3.3.2 Monitoring cell behavior during drug treatment

After cells were seeded on the sensor surface as explained in Section 2.2.2.3, they were replaced into the QCM-D chamber. The change in QCM-D signals caused by the cell reactions during the drug treatments was presented in Figure 3.5. When the stable baseline for both frequency and dissipation signals at the third harmonics was obtained, the medium containing HER2-mAb was pumped to the measurement chamber until the whole chamber was filled (ca. 10 min). After 10 minutes, the flow was stopped, and cells were incubated with medium containing HER2-mAb under no-flow conditions approximately for 75 minutes to observe the effect of drug presence. The response of SKOV-3 cells to HER2-mAb at different concentrations, i.e. 40, 80, 120, and 160 µg/mL, can be seen in Figures 3.5C, D, E, F, and Appendix C, Figure C2, respectively. While there was a noticeable increase in frequency, a distinctive decrease in dissipation was observed in drug treatment experiments. There was almost no change in QCM-D signals in control experiments. This means that the HER2-mAb targeted drug binds to HER2 receptors of SKOV-3 cells and triggers several intracellular events that result in morphological changes as can be seen in Figure 3.7C, D, E, F. Furthermore, these morphological changes lead to frequency and dissipation change that is detectable by QCM-D.

Dynamic cytoskeleton modifications in the mechanical phenotype of the cells can be triggered with either extracellular or intracellular events [94]. These changes are the result of cellular processes that affect cell assembly and morphogenesis, motility, and mitosis [95]. To analyze this dynamic cytoskeleton and morphologic changes of the cells, QCM-D is a good alternative since even a small change in the cell-surface interface can be detected without any label. Moreover, several studies show alterations in the biophysical features of the cells such as stiffness, elasticity, and adhesion can be measured by QCM-D [73, 76, 96].

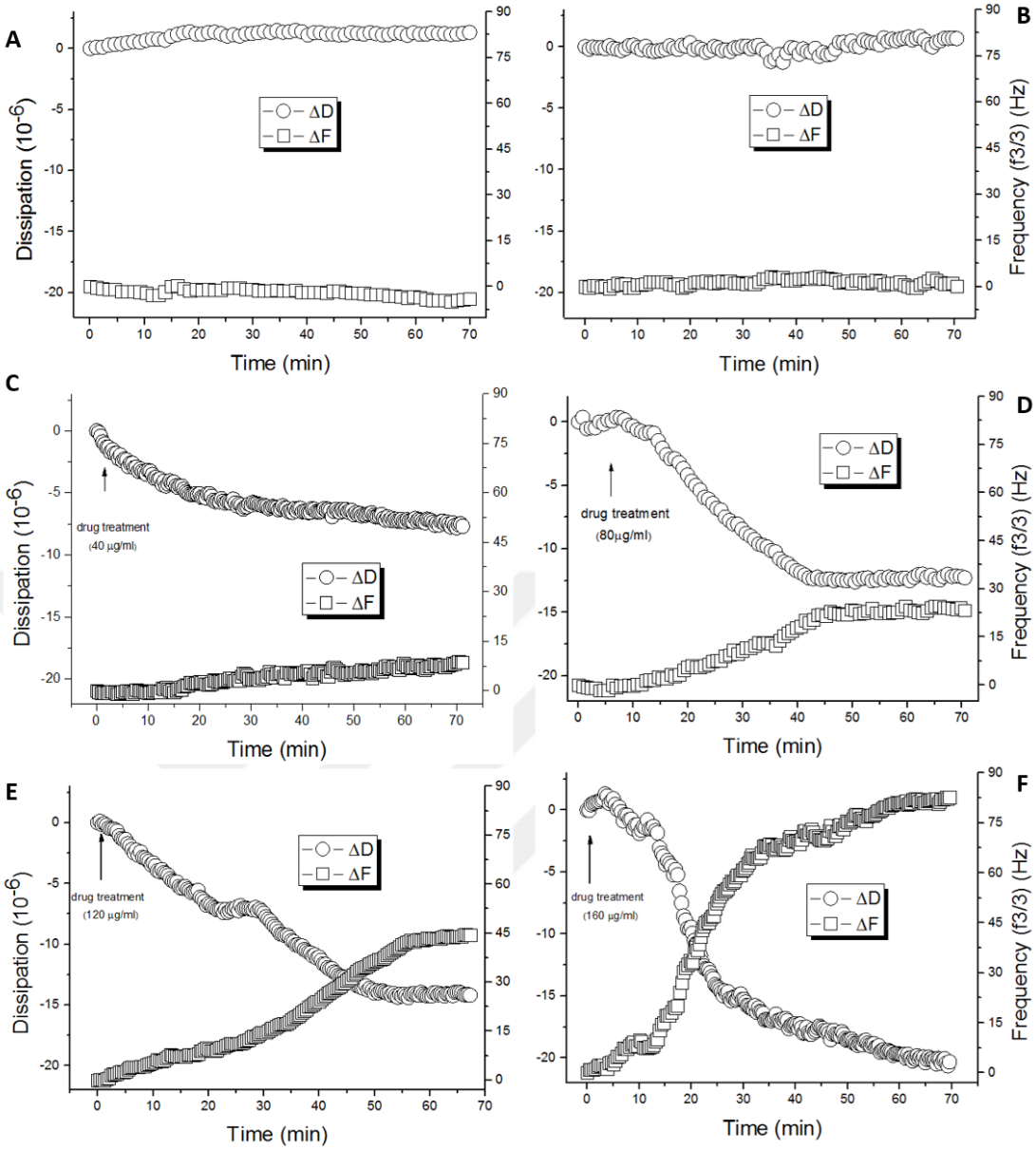


**Figure 3.5 :** QCM-D signals versus time monitored on cell seeded gold sensor during drug treatment. Square shapes indicate Δf, round shapes indicate ΔD. The behavior of untreated (A) and (B) and HER2-mAb treated; (C) 40, (D) 80, (E) 120, and (F) 160 µg/mL; cells were followed by the change in Δf and ΔD.

As can be in Figure 3.5C, D, E, F, when the drug dose was increased, an increase in frequency value was observed. Frequency signals in QCM-D are a linear function of the adsorbed mass (Δm) on the sensor surface. When the adsorbed mass on the sensor surface increases, the frequency decreases, and vice versa, if the frequency increases which means the adsorbed mass on the sensor surface decreases[73].

In addition to those noticeable changes in Δf and ΔD signals, drug concentration also caused a significant change in acoustic ratio values (Figure 3.6) which are related to the viscoelastic properties of the cell layer. Using acoustic ratio is convenient to

directly compare the energy losses per unit mass on the surface[97]. The comparatively high acoustic ratio values state very viscoelastic cell layers. Therefore the decrease in the acoustic ratio can be explained as an increment in rigidity at the interfacial layer of the cells [70].

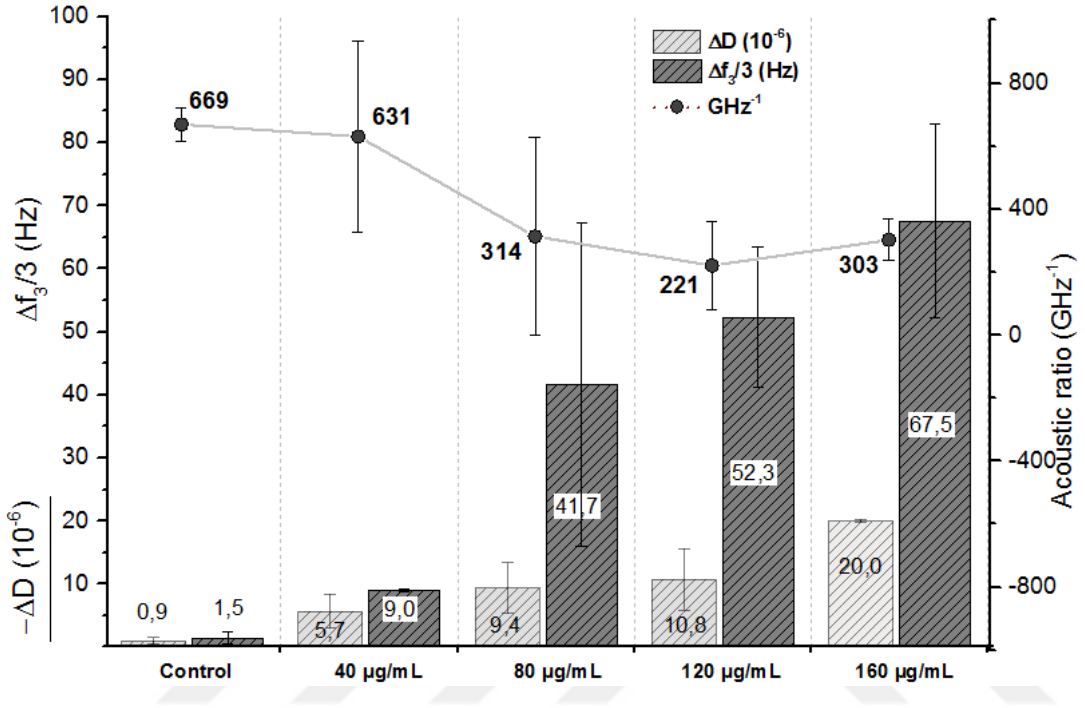


**Figure 3.6 :** Frequency (Δf), dissipation (-ΔD) and acoustic ratio values at the end of 1.5 h that stable baseline values before treatment and after treatment.

### 3.4 Microscopy Images of Cells treated with Drug

Changes in cell morphology are controlled by cell signaling pathways that can be initiated by external or internal stimuli[85]. To observe the morphology changes after HER2 targeted drug treatment, cells were fixed as explained in Section 2.2.3.1, and images of cells were taken by fluorescence microscopy (Figure 3.7). To mimic the QCM-D conditions, cells were incubated on gold sensors for 1.5 hours at 37°C and under no-flow and treated with the HER2-mAb with 40, 80, 120, and 160 µg/mL concentrations same as in QCM-D experiments.

To visualize the cell morphologies and spreading, cells stained with the Phalloidin dye. Phalloidin is a highly selective bicyclic peptide that binds to all variants of actin filaments in various species of animals and plant cells[98]. Actin filaments are especially plenty beneath the plasma membrane[80], where they create a network of actin and actin-binding proteins. Actin filament and the other cytoskeleton components

like microtubules and intermediate filaments controls cell shape organizations and helps the movement of the cell on the surfaces, so make possible to cells migration, engulf particles, and cell division[80, 95, 99]. In our experiments, noticeable changes in the cell morphologies and cell spreading surface area were observed with the increased drug concentration. In Bianco's study[94], these kind of changes triggered by a drug treatment were the result of specific molecular alterations induced by regulations of expression of actin-binding proteins. Thus, it can be said that the change in the morphology and spreading of the cells can be triggered by drug binding.

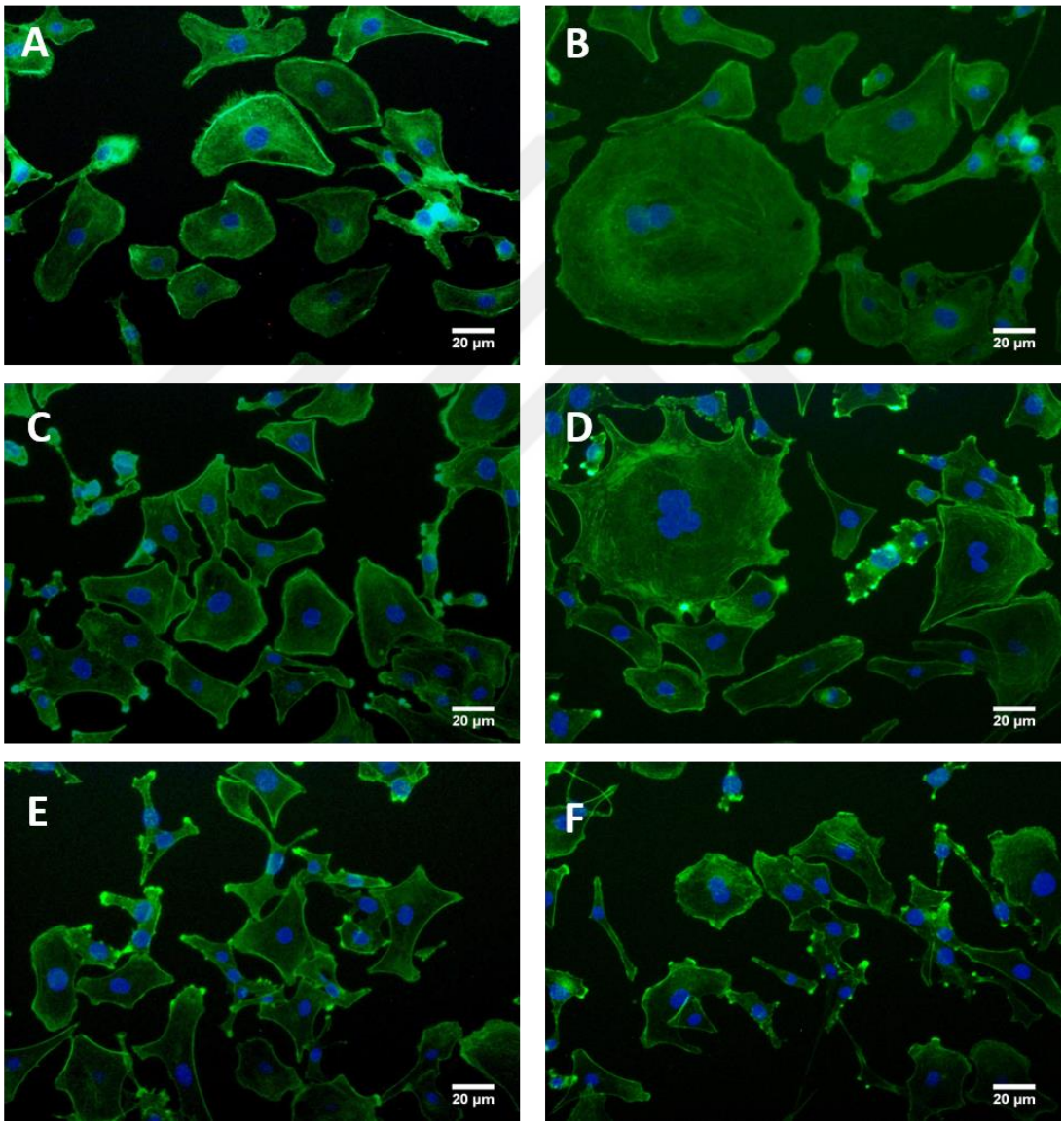


**Figure 3.7 :** Investigation of morphology of cells incubated with HER2-mAb containing in serum-free medium. (under 20x) (blue: DAPI; green: Phalloidin CruzFluor). (A) and (B) images belong to control experiments that cells were incubated with HER2-mAb free media. (C) 40, (D)80, (E)120, and (F) 160 µg/mL HER2-mAb concentrations that cells treated.

The effect of the drug on the cell morphology becomes visible at 40 µg/mL drug (Figure 3.7C) and more pronounced as concentration increased (Figures 3.7 D-F). When the morphology of the drug-treated cells (i.e Figure 3.7D) compared to that of the control cells (i.e Figure 3.7B), a significant effect on the cell shapes can be observed. While the shape of the control cells was smooth, the shapes of the drug-treated cells become more curled after treatment. On the other hand, the edges of the cells incubated with the drug are more intensely stained with Phalloidin. Intensely stained cell edges can be explained by the increased concentration of actin filaments at the cell edges. These dense actin filaments would lead to a change in cell shape and more rigid cell edges. When drug dose was increased, the intensely stained cell morphologies were increased as seen in Figure 3.7.

### 3.5 Interpretation of QCM-D Data Together with Microscopy Images

Both the QCM-D and fluorescent microscopy images showed that HER2-mAb binding triggers the change in morphology of the cells. As can be seen in Figure 3.7C, D, E, F, especially in Figure 3.7D, cell edges lost their smooth shape and become more curled, and therefore cell surface area and adsorbed mass were decreased. It can be said that these decreases in the surface area led to an increase in the frequency signal of QCM-D.

Furthermore, when the drug dose was increased, a decrease in dissipation value was observed (Figure 3.5C, D, E, F) which can be interpreted as the loss of elasticity of cells as a response to HER2-mAb binding. As can be seen in fluorescent microscopy images in Figure 3.7C, D, E, F, the edges of the cells incubated with the drug are more intensely stained. Intensely stained cell edges can be explained by the increased concentration of actin filaments at the cell edges. As actin filaments are highly flexible: are arranged and removed simply, and are related with each other in several ways[79], binding of the drug to SKOV3 cells, may lead to increase actin filaments concentration and change the distribution of actin filaments around the cell edges. These reorganizations of actin filaments would lead to an increase in cell rigidity and this explains the decrease in dissipation values.

Moreover, other QCM-D studies in the literature investigate the drug effects on living cells. According to Zhang's resveratrol (antineoplastic agent, has potential in the remedy of various types of cancer cell [76]) treatment on MC-7 cells (breast cancer

cell line[100]) [76], decrease in dissipation value was observed with the increasing drug concentration consistent with our results. This decrease in dissipation was explained by the loss of elasticity of cells which would cause the increasing stiffness of the cell matrix[76, 94]. Matrix stiffness, i.e. resistance to deformation, is one of the many mechanical responses shown by cells and it is a crucial mediator of cell behavior [101]. Although different cell types and different compounds were used, the decrease in dissipation may lead to stiffness of the cells

## 4. CONCLUSIONS

In conclusion, QCM-D is a good alternative to analyze real time bioactivity properties of mAbs and it can detect any small change in the cell-surface interface without any label. Therefore, QCM-D enables detecting dynamic cytoskeleton modifications in the mechanical phenotype of the cells that triggered with mAb binding. QCM-D provides a real-time ligand binding assays to studyi drug binding activities. Unlike the other biosensors that use purified and immobilized target molecules, it enables to work directly with cells and their receptors in their native environment. For future works, this ligand binding assay that we developed can be used for new assays that applicable to different QCM-D systems and used drug concentrations can be reduced. New assays can be developed based on our work.

## REFERENCES


**[1] Maverakis, Emanual**, (2015). Glycans In The Immune system and The Altered Glycan Theory of Autoimmunity: A Critical Review, *J Autoimmun.*, 0:1:13.

**[2] Diagnostics, Creative,** (2020). Polyclonal vs. Monoclonal Antibodies, Available at https://www.creative-diagnostics.com/polyclonal-vs-monoclonal-antibodies.htm, Cited on 03.05.2020.

**[3] Skottrup, P. D., Nicolaisen, M., Frokiaer, H., and Justesen, A. F.**, (2007). Monoclonal antibody-based Surface Plasmon Resonance sensors for pathogen detection, *Technical University of Denmark.*

**[4] KABAT, A. E.**, (1980). Basic principles of antigen-antibody reactions, *METHODS IN ENZYMOLOGY*, 70:3:49.

**[5] Lu, Ruei-Min,** (2020). Development of therapeutic antibodies for the treatment of diseases, *Journal of Biomedical Science*, 27:2:30.

**[6] Hendriksen, Marlies Leenaars and Coenraad F. M.**, (2005). Critical Steps in the Production of Polyclonal and Monoclonal Antibodies: Evaluation and Recommendations, *ILAR Journal*, 46:269:279.

**[7] Kohler, G.; Milstein, C**., (1975). Continuous Cultures of Fused Cells Secreting Antibody of Predefined Specificity, Nature, 256:495:497.

**[8] NobelPrize.org,** (1984). The Nobel Prize in Physiology or Medicine, Available at https://www.nobelprize.org/prizes/medicine/1984/summary/, Cited on 02.05.2020.

**[9] Immunology.org,** (1975). Kohler and Milstein's hybridoma technology. Available at https://www.immunology.org/kohler-and-milsteins-hybridoma-technology-1975. Cited on 02.05.2020.

**[10] PhRMA**, (2015). Pharmaceutical Research and Manufacturers of America. Medicines in development: Biotechnology. Available at http://phrma-docs.phrma.org/sites/default/files/pdf/2015_phrma_profile.pdf. Citen on 05.05.2020.

**[11] Covic, A., Andia, J. C., and Cancarini, G.**, (2008). Biosimilars and biopharmaceuticals: what the nephrologists need to know—a position paper by the ERA-EDTA Council, *Nephrol Dial Transplant*, 23:3731–3737.

**[12] Rader, Ronald A,** (2008). (Re)defining biopharmaceutical, *Nature Biotechnology* 26:743:751.

**[13] Vulto, A. G. and Jaquez A. O.**, (2017). The process defines the product: what really matters in biosimilar design and production?, *Rheumatology*, 56:14:29.

**[14] Declerck, P.,** (2012). Biologicals and biosimilars: a review of the science and its implications, *Generics and Biosimilars Initiative Journal (GaBI J)*, 1:13:6.

**[15] Rodrigues, H. L., Carneiro, A. V. and Cabrita A.,** (2009). Position statement of the Portuguese Society of Nephrology on the clinical use of

biotechnological drugs in renal patients, *Port J Nephrol Hypert*, 4:317-321.

**[16] Buettner, M. J., Shah, S. R. and Saeui C. T.,** (2018). Improving Immunotherapy Through Glycodesign, *Frontiers in Immunology*, 2:1:8.

**[17] Sciences, MBL Life,** (2020). Structure and characteristics of antibody isotypes. Available at https://ruo.mbl.co.jp/bio/e/index.html, Cited on 02.05.2020.

**[18] Humphrey, Samuel Scott Perdue and John H.,** (2020). Immune system, Encyclopædia Britannica, inc., Available at https://www.britannica.com/science/immune-system, Cited on 03.05.2020,

**[19] Antibody Isotypes & Subtypes,** Website Name: Absolute Antibody URL: https://absoluteantibody.com/antibody-resources/antibody-overview/antibody-isotypes-subtypes/ Access Date: May 03, 2020.

**[20] Janeway C.A., Travers P., Walport M.,** (2001). Immunobiology: The Immune System in Health and Disease, Available from https://www.ncbi.nlm.nih.gov/books/NBK27144/, *New York: Garland Science*, 5th edition.

**[21] Stadlmann, J., Pabst, M., Kolarich, D., Kunert, R. and Altmann, F.,** (2008). Analysis of immunoglobulin glycosylation by LC-ESI-MS of glycopeptides and oligosaccharides, *Proteomics*, 8:2858–2871.

**[22] Janeway, C. A,** (2001). Immunobiology, Garland Publishing.

**[23] Lumen,** (08.03.2020). The Adaptive Immune Response: B-lymphocytes and Antibodies, *Chapter 11: The Lymphatic and Immune System*, avalaible at https://courses.lumenlearning.com/nemcc-ap/chapter/the-adaptive-immune-response-b-lymphocytes-and-antibodies/.

**[24] Creative Biolabs,** (02.06.2020). Native™ Human Antibody Discovery Service, Available at https://www.creative-biolabs.com/Native-TM-Human-Antibody-Discovery-Service.html.

**[25] Mallbris, Lotus,** (2016). Molecular Insights into Fully Human and Humanized Monoclonal Antibodies, *The Journal of clinical and aesthetic dermatology*, 9:13:15.

**[26] Owens, R. J. and Young, R. J.,** (1994). The genetic engineering of monoclonal antibodies, *Journal of Immunological Methods*, 168:149-165.

**[27] Caspi, Rachel R.,** (2008). Immunotherapy of autoimmunity and cancer: the penalty for success, *Nat Rev Immunol.*, 8:970:976.

**[28] Baxter, D.,** (2007). Active and passive immunity, vaccine types, excipients and licensing, *Occupational Medicine*, 57:552:556.

**[29] Attarwala, Husain,** (2010). Role of antibodies in cancer targeting, *Journal of natural science, biology, and medicine*, 1:53:56.

**[30] Ho, Mitchell,** (2018). Inaugural Editorial: Searching for Magic Bullets, *Antibody Therapeutics*, 1:1-5.

**[31] Smith, Mitchell R,** (2003). Rituximab (monoclonal anti-CD20 antibody): mechanisms of action and resistance, *Oncogene*, 22:7359:7368.

**[32] Hendriks, D., Choi, G. and Bruyn, M.,** (2017). Antibody-Based Cancer Therapy: Successful Agents and Novel Approaches, *International Review of Cell and Molecular Biology*, 331:290:337.

**[33] Wong, Siu-Fun,** (2005). Cetuximab: An epidermal growth factor receptor monoclonal antibody for the treatment of colorectal cancer, *Clinical Therapeutics*, 27:684:694.

**[34] Constantine, Zahi Mitri and Tina,** (2012). The HER2 Receptor in Breast Cancer: Pathophysiology, Clinical Use, and New Advances in Therapy, *Chemotherapy Research and Practice*, 743193.

**[35] Shaker Abuharbeid, Jürgen Apel,** (2005). Inhibition of HER-2 by three independent targeting strategies increases paclitaxel resistance of SKOV-3 ovarian carcinoma cells, *Naunyn-Schmiedeberg's Archives of Pharmacology*, 371:141:151.

**[36] Serrano-Olvera A, Duenas-Gonzalez A, Gallardo-Rincon D.,** (2006). Prognostic, predictive and therapeutic implications of HER2 in invasive epithelial ovarian cancer. , *Cancer Treat Rev.*, 32:180:190.

**[37] Albano, Alessandra Magnifico and Luisa,** (2009). Tumor-Initiating Cells of HER2-Positive Carcinoma Cell Lines Express the Highest Oncoprotein Levels and Are Sensitive to Trastuzumab, *Cancer Therapy: Preclinical*, 15:2010:2021.

**[38] Wang, Lin Yu and Yuxi,** (2014). Eradication of Growth of HER2-Positive Ovarian Cancer With Trastuzumab-DM1, an Antibody-Cytotoxic Drug Conjugate in Mouse Xenograft Model, *Int J Gynecol Cancer*, 24:1158:1164.

**[39] Cancer Treatment;** targeted therapy, Website Name: Cancer clinics, URL: https://www.cancerclinics.in/treat-cancer Access Date: May 03, 2020.

**[40] Molina, M. A., Jordi Codony-Servat, J. and Albanell, J.,** (2001). Trastuzumab (Herceptin), a Humanized Anti-HER2 Receptor Monoclonal Antibody, Inhibits Basal and Activated HER2 Ectodomain Cleavage in Breast Cancer Cells, *CANCER RESEARCH*, 61:4744–4749.

**[41] Yarden, Yosef,** (2001). Biology of HER2 and Its Importance in Breast Cancer, *Oncology*, 2:1:13.

**[42] M., Nowicki,** (2007). Basic Facts about Biosimilars, *Kidney Blood Press Res*, 30:267:272.

**[43] Singh, Rajiv Kumar and Jagjit,** (2014). Biosimilar drugs: Current status, *Int J Appl Basic Med Res.*, 4:63:66.

**[44] Wang, X., An, Z., and Luo, W.,** (2018). Molecular and functional analysis of monoclonal antibodies in support of biologics development, *Protein Cell*, 9:74–85.

**[45] Wang, Weihong,** (2014). Potency Testing of Biopharmaceutical Products, *AMERICAN PHARMACEUTICAL REVIEW, Available at* https://www.americanpharmaceuticalreview.com/Featured-Articles/169473-Potency-Testing-of-Biopharmaceutical-Products/, *Cited on 05.05.2020*.

**[46] Biolabs, Pacific,** (2020). In Vitro Potency Assays. Available at https://pacificbiolabs.com/in-vitro-potency-assays, Cited on 25.05.2020.

**[47] Lequin, Rudolf M,** (2005). Enzyme Immunoassay (EIA)/Enzyme-Linked Immunosorbent Assay (ELISA) *Clinical Chemistry*, 51:2415–2418.

**[48] Judy Gibbs, Michelle Vessels, and Mark Rothenberg,** (2020). Selecting the Detection System – Colorimetric, Fluorescent, Luminescent Methods for ELISA Assays - Application Note. Available at

https://www.biosigma.it/data/pdf_guides/en/CLS-DD-AN-458.pdf, Cited on 26.05.2020.

**[49] Neubig, R. R., Spedding, M., and Pedding, T. K.,** (2003). International Union of Pharmacology Committee on Receptor Nomenclature and Drug Classification. XXXVIII. Update on Terms and Symbols in Quantitative Pharmacology, *Pharmacol Rev.*, 55:597:606.

**[50] Helmerhorst, E., Chandler, D. J., Nussio, M., and Mamotte, C. D.,** (2012). Real-time and Label-free Bio-sensing of Molecular Interactions by Surface Plasmon Resonance: A Laboratory Medicine Perspective., *The Clinical Biochemist. Reviews*, 33:161:173.

**[51] Homola, Jir,** (1999). Surface plasmon resonance sensors: review, *Sensors and Actuators*, 54:3:15.

**[52] Robert Karlsson, Anne Michaelsson and Lars Mattsson**, (1991). Kinetic analysis of monoclonal antibody-antigen interactions with a new biosensor based analytical system, *Journal of Immunological Methods*, 145:229:240.

**[53] Shinn-Fwu Wang, Hung-Shing Tsai,** (2013). Improved Small-Angle Sensor Based on Total-Internal Reflection and Surface Plasmon Resonance in Heterodyne Interferometry, *Sensors and Materials*, 25:417:422.

**[54] Pattnaik, Priyabrata,** (2005). Surface plasmon resonance; Applications in understanding receptor-ligand interaction, *Applied Biochemistry and Biotechnology*, 126:79:92.

**[55] Hutchinson, Andrew M.,** (1995). Evanescent Wave Biosensors Real-Time Analysis of Biomolecular Interactions, *Moleculer Biotechnolgy*, 3:47:54.

**[56] WHO Expert Committee,** (2013). Guidelines on evaluation of similar biotherapeutic products (SBPs), sixtieth report, *WHO Expert Committee on Biological Standardization*, Annex 2:accessed 18.03.2020.

**[57] Genentech,** (2019). Avastin Prescribing Information. Available at https://www.gene.com/download/pdf/avastin_prescribing.pdf, Cited on 26.05.2020.

**[58] Birbrair A, Zhang T, Wang ZM, Messi ML, Mintz A, Delbono O,** (2015). Pericytes at the intersection between tissue regeneration and pathology, *Clinical Science*, 128:81:93.

**[59] Avastin,** (2020). About Avastin: Proposed Mechanism of Action, Available at https://www.avastin.com/hcp/mcrc/proposed-moa.html, Cited on 26.05.2020.

**[60] Hansel TT, Kropshofer H, Singer T, Mitchell JA, George AJ,** (2010). The safety and side effects of monoclonal antibodies, *Nat Rev Drug Discov*, 9:325:338.

**[61] Reviakine, I., Johannsmann, D. & Richter, R.P.,** (2011). Hearing what you cannot see and visualizing what you hear : interpreting quartz crystal microbalance data from solvated interfaces., *Anal Chem*, 83:8838:8848.

**[62] Richter, Natalia S. Baranova & Ralf P.,** In situ Physico-Chemical Characterization of Surface Confined Supramolecular Assemblies. Available at https://www.glycopedia.eu/e-chapters/in-situ-physico-chemical/Quartz-Crystal-Microbalance-with, Cited on 24.05.2020.

**[63] Dixon, M. C. ,** (2008). Quartz crystal microbalance with dissipation monitoring: enabling real-time characterization of biological materials and their interactions, *Journal of Biomolecular Techniques*, 19:151:158.

**[64] NanoScience Instruments,** (24.05.2020). Quartz Crystal Microbalance (QCM), Available at https://www.nanoscience.com/techniques/quartz-crystal-microbalance/.

**[65] Jun Xi, Jennifer Y. Chen, Marcela P. Garcia and Lynn S. Penn,** (2013). Quartz Crystal Microbalance in Cell Biology Studies, *Biochips & Tissue Chips*, S5:2:9.

**[66] Sauerbrey, G.**, (1959). Verwendung von Schwingquarzen zur Wägung dünner Schichten und zur Mikrowägung. [Use of quartz crystal units for weighing thin films and Microweighing], *Zeitschrift für Physik*, 155:206-222.

**[67] Viitala, T. ,** (2005). Modeling the Mechanical Properties of Adsorbed Deposited Layers At Air-Solid And Liquid-Solid Interfaces With The Dissipative KSV QCM-Z500 *KSV Instruments Ltd., Helsinki*, 1:33.

**[68] Amitava Dasgupta, Amer Wahed,** (2014). A Comprehensive Review for Board Preparation, Certification and Clinical Practice - Laboratory Statistics and Quality Control, *Clinical Chemistry, Immunology and Laboratory Quality Control*, Chapter 4:47-66.

**[69] Hillier AC, Ward MD,** (1992). Scanning electrochemical mass sensitivity mapping of the quartz crystal microbalance in liquid media, *Anal Chem*, 64:2539:2554.

**[70] Kılıc, A. and Kok, F. N.,** (2018). Quartz crystal microbalance with dissipation as a biosensing platform to evaluate cell–surface interactions of osteoblast cells, *Biointerphases*, 13:1:9.

**[71] Hattori, T. Nomura and O.,** (1980). Determination of micromolar concentrations of cyanide in solution with a piezoelectric detector, *Analytica Chimica Acta*, 115:323:326.

**[72] Cooper, M. A., & Singleton, V. T. ,** (2007). A survey of the 2001 to 2005 quartz crystal microbalance biosensor literature: applications of acoustic physics to the analysis of biomolecular interactions, *J Mol Recognit*, 20:154:184.

**[73] Kılıc, A.,** (2018). Construction and Characterization of solid-supported Lipid Bilayers to Investigate Cell-Surface Interactions, *Istanbul Technical University, Department of Molecular Biology-Genetics and Biotechnology*.

**[74] Hook, F. ,** (2001). Variations in coupled water, viscoelastic properties, and film thickness of a Mefp-1 protein film during adsorption and cross-linking : a quartz crystal microbalance with dissipation monitoring, ellipsometry, and surface plasmon resonance study, *Anal Chem*, 73:5796-5804.

**[75] Elmlund, L., Kack, C., Aastrup, T. & Nicholls, I. A. ,** (2015). Study of the Interaction of Trastuzumab and SKOV3 Epithelial Cancer Cells Using a Quartz Crystal Microbalance Sensor, *Sensors, 15, 5884-5894*.

**[76] Bai, Shaolian Zhang and Haihua,** (2015). Label-Free Quartz Crystal Microbalance with Dissipation Monitoring of Resveratrol Effect on Mechanical Changes and Folate Receptor Expression Levels of Living MCF-7 Cells: A Model for Screening of Drugs, *Anal. Chem.*, 87:4797:4805.

**[77] Wegener J, Janshoff A, Galla HJ,** (1998). Cell adhesion monitoring using a quartz crystal microbalance: comparative analysis of different mammalian cell lines, *Eur Biophys J* 28:26:37.

**[78] Geiger T, Zaidel-Bar R,** (2012). Opening the floodgates: proteomics and the integrin adhesome. , *Curr Opin Cell Biol*, 24:562:568.

**[79] The cell,** (2019). 7. Cytosol. Cytoskeleton. ACTIN FILAMENTS 19.05.2020 Available at https://mmegias.webs.uvigo.es/02-english/5-celulas/7-actina.php, *Atlas of plant and animal histology*.

**[80] GM., Cooper,** (2000). Structure and Organization of Actin Filaments, *The Cell: A Molecular Approach. 2nd edition, Sunderland (MA): Sinauer Associates, Available from:* https://www.ncbi.nlm.nih.gov/books/NBK9908/,

**[81] Wozniak MA, Modzelewska K, Kwong L, Keely PJ** (2004). Focal adhesion regulation of cell behavior, *Biochim Biophys Acta* 1692:103:119.

**[82] Michelini, E.; Cevenini, L.; Mezzanotte, L.; Coppa, A.; Roda, A.,** (2010). Cell-based assays: Fuelling drug discovery, *Anal. Bioanal. Chem.*, 398:227–238.

**[83] Tothill, I.E.,** (2009). Biosensors for cancer markers diagnosis, *Semin. Cell Dev. Biol.*, 20:55:62.

**[84] Hawkins, E.; Cooper, M.; Campbell, I. ,** (2006). Acoustic detection technology in the analysis of biomolecular interactions, *Innov. Pharm. Technol.*, 21:30-34.

**[85] Tymchenko, N., Nileback, E.,** (2012). Reversible Changes in Cell Morphology due to Cytoskeletal Rearrangements Measured in Real-Time by QCM-D, *Biointerphases*, 7:43.

**[86] Peiris, D.; Markiv, A.; Curley, G.P.; Dwek, M.V. ,** (2012). A novel approach to determining the affinity of protein–carbohydrate interactions employing adherent cancer cells grown on a biosensor surface, *Biosens. Bioelectron.* , 35:160:166.

**[87] Hong, C., Lee, J., Zheng, H., Hong, S. S. & Lee., C.,** (2011). Porous silicon nanoparticles for cancer photothermotherapy, *Nanoscale Res. Lett.*, 6:321.

**[88] Merck,** (2013). Fundamental Techniques in Cell Culture Laboratory Handbook, 4th Edition, European Collection of Authenticated Cell Cultures.

**[89] Fredriksson, C., Kihlman, Rodahl, S. M., and Kasemoon, B.,** ( 1998). The Piezoelectric Quartz Crystal Mass and Dissipation Sensor: A Means of Studying Cell Adhesion, *Langmuir*, 14: 248:251.

**[90] Yang, Z. and Xiong, H. R,** (2012). Culture Conditions and Types of Growth Media for Mammalian Cells, *Biomedical Tissue Culture, Intech Open, 1.Edition*.

**[91] Chemicals, Hopax Fine,** (2018). Biological buffers and their interactions with metal ions, Available at https://www.hopaxfc.com/en/blog/biological-buffers-and-their-interactions-with-metal-ions, Cited on 25.04.2020.

**[92] Attar, R., Cincin, Z. B., Bireller, E. S., and Cakmakoglu, B.,** (2017). Apoptotic and genomic effects of corilagin on SKOV3 ovarian cancer cell line, *OncoTargets and Therapy*, 10:1941:1946.

**[93] Gori, G. B.,** (1964). Trypsinization of Animal Tissues for Cell Culture: Theoretical Considerations and Automatic Apparatus, *APPLIED MICROBIOLOGY*, 12:115:121.

**[94] Bianco, M. and Vergara, D.,** (2018). Quartz Crystal Microbalance as Cell-Based Biosensor to Detect and Study Cytoskeletal Alterations and Dynamics, *Biotechnol. J.*, 1700699:1:9.

**[95] Pollard, T. D. and Borisy, G. G.,** (2003). Cellular motility driven by assembly and disassembly of actin filaments, *Cell*, 112:453-465.

**[96] Chikkaveeraiah, Ashwinkumar A. Bhirde and Bhaskara V.,** (2014). Targeted Therapeutic Nanotubes Influence the Viscoelasticity of Cancer Cells to Overcome Drug Resistance, *ACS Nano*, 8:4177:4189.

**[97] Feiler, A. A., Sahlholm, A., Sandberg, T., & Caldwell, K. D.,** (2007). Adsorption and viscoelastic properties of fractionated mucin (BSM) and bovine serum albumin (BSA) studied with quartz crystal microbalance (QCM-D), *J Colloid Interface Sci*, 2:475-481.

**[98] Abcam,** (19.05.2020). Phalloidin staining protocol, Available at https://www.abcam.com/protocols/phalloidin-staining-protocol.

**[99] Engqvist-Goldstein, A.E. and Drubin, D. G.,** (2003). Actin assembly and endocytosis: from yeast to mammals, *Annu. Rev. Cell Dev. Biol.*, 19:287:332.

**[100] Adrian V. Lee, Steffi Oesterreich, Nancy E. Davidson,** (2015). MCF-7 Cells—Changing the Course of Breast Cancer Research and Care for 45 Years, *Journal of the National Cancer Institute*, 107:1:4.

**[101] Wells, R. G. ,** (2008). The Role of Matrix Stiffness in Regulating Cell Behavior, *Hepatology* 47:1394:1400.

## APPENDICES

**APPENDIX A :** Laboratory Equipment

Pipettes (Eppendorf 10µl, 100 µl, 1000 µl, 2500 µl, 5000 µl)

pH meter (Hanna Instruments, HI 9124)

Magnetic stirrer (Cole-Parmer, Stable Temp)

Bath Sonicator (Transsonic TP 690)

UV-Ozone System (Novascan, PSD Pro Series)

QCM-Z500 (KSV Instruments)

Optic Microscopy (Olympus)

Fluorescence Microscopy (Zeiss axiovert a.1 inverted)

Tubing (Tygon, SC0060; R3607)

Peristaltic pump

QCM slides (Q-Sense, Sweden)

Laminar Air Flow Cabinets (FASTER BH-EN 2003)

Electronic Pipette (CappAid)

Centrifuge (Scanspeed 1730 R)

Incubator with CO2 (BINDER)

Hemacytometer (Isolab)

Freezers (Altus ( +4°C)) (Siemens ( -20°C))

Falcons (15 ml, 50 ml) (Isolab)

12-well F plate (TPP)

Serological pipettes Sarstedt

Eppendorf tubes (2ml) (Interlab)

**APPENDIX B:** Chemicals

PBS (Phosphate buffered saline) (Adjust pH 7.4 with HCl or NaOH)

- 1.78 g Na2HPO4.2H20

- 0.27 g KH2PO4

- 0.20 g KCl

- 8 g NaCl in 1 liter

Ethanol (Sigma, 32221-SL)

Sodium Chloride

Potassium Chloride

Sodium Hydroxide

Hydrochloric Acid

Potassium Dihydrogenphosphate (KH2PO4)

Disodium Hydrogen Phosphate Dihydrate (Na2HPO4.2H2O)

SDS (sodium dodecyl sulfate)

Fetal Bovine Serum (FBS) (10%) (Gibco)

Penicillin/Streptomycin (1%) (Gibco)

Trypan Blue (Lonza)

DMSO (Fisher-Scientific)

Formaldehyde

Triton® X-100

4′,6-diamidino-2-phenylindole dihydrochloride (DAPI; 100nM)

Bovine Serum Albumin

Phalloidin CruzFluor™ 488 Conjugate (Excitation/Emission wavelength 493/517 nm) (Santa Cruz)

Purified water (minimum resistivity of 18.2 MΩ.cm)

Ammonia ($NH_3$)

Hydrogen peroxide ($H_2O_2$)

4-(2-hydroxyethyl)-1-piperazineethanesulfonic acid (HEPES)

**APPENDIX C :** Supplementary Images and Graphs

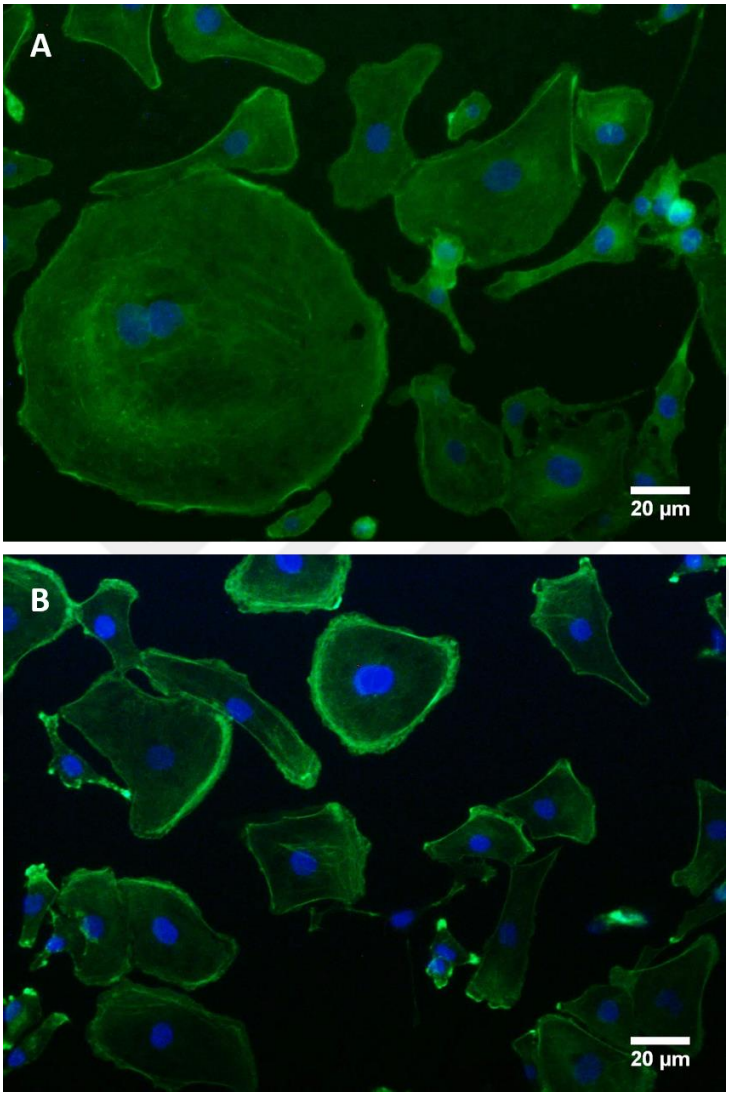


**Appendix C.1:** Morphology of cells incubated in serum-free [A] and serum-supplemented [B] medium for 1.5 hours the same as drug treatment time. Fluorescence microscopy images of 0.5.105 cells in CO2 independent medium (under 20x) (blue: DAPI; green: Phalloidin CruzFluor)

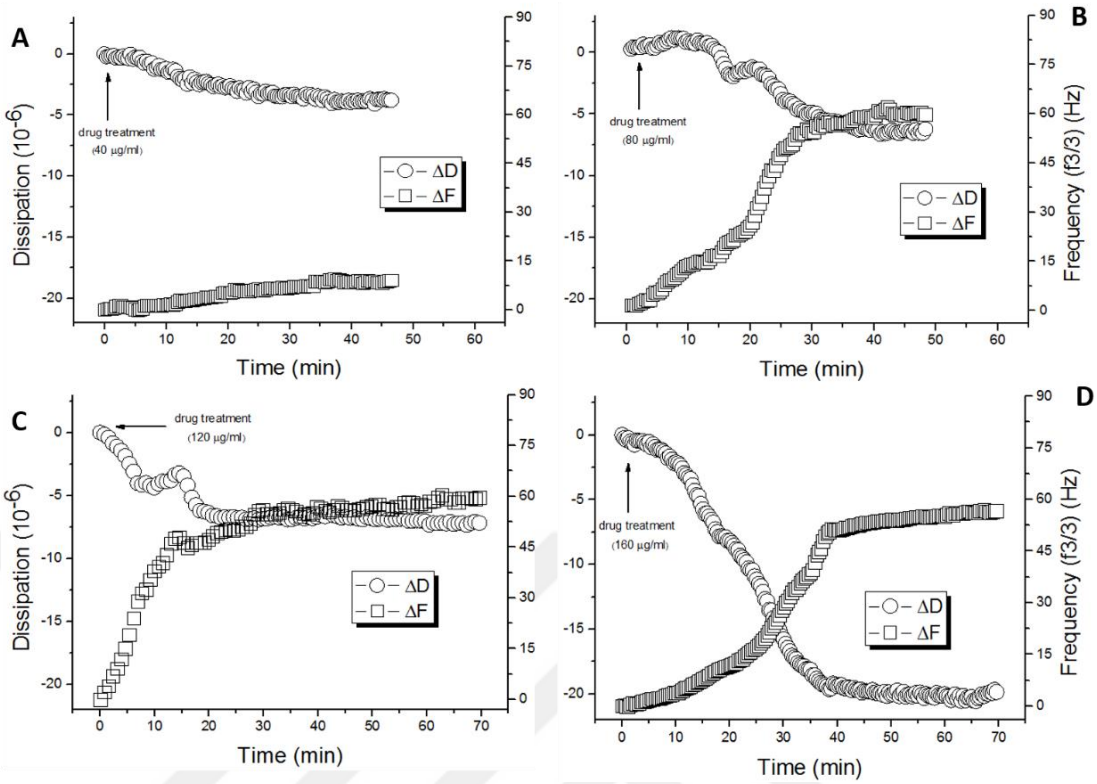


**Appendix C.2 :** QCM-D signals versus time monitored on cell seeded gold sensor during drug treatment. Square shapes indicate Δf, round shapes indicate ΔD. The behavior of HER2-mAb treated; (A) 40, (B) 80, (C) 120, and (D) 160 µg/mL; cells were followed by the change in Δf and ΔD.

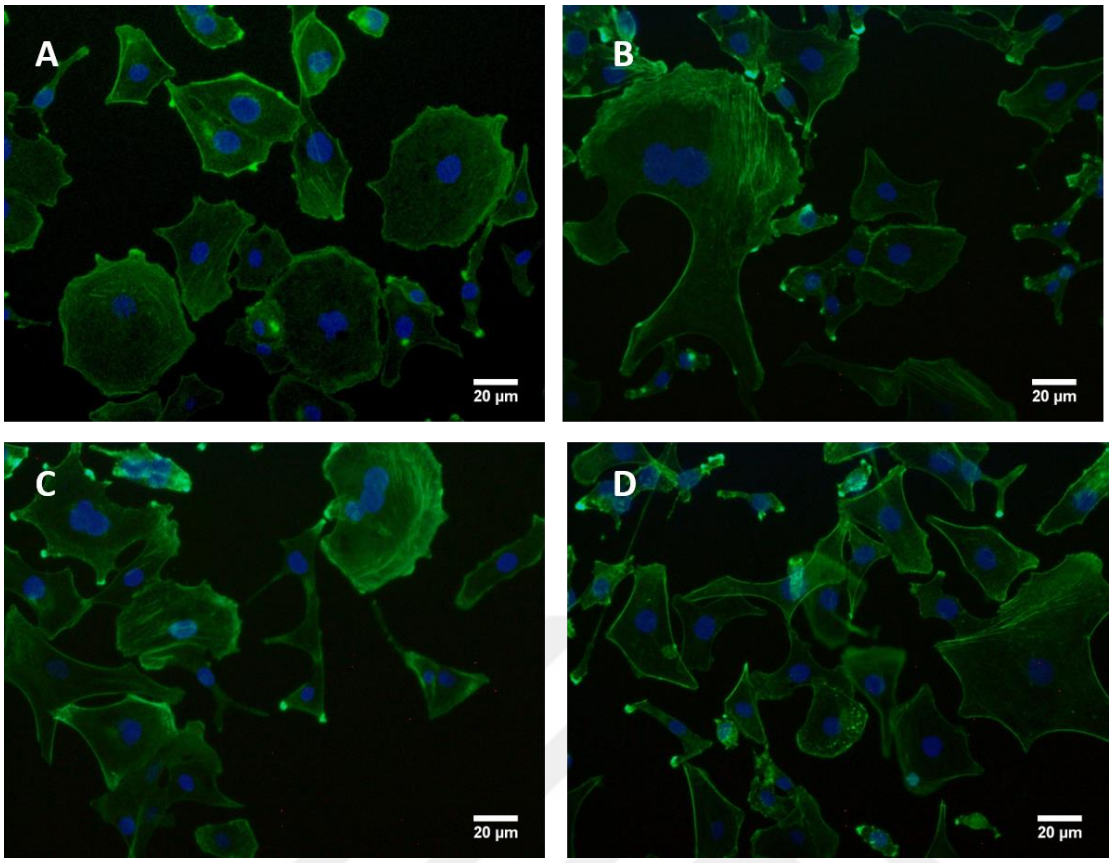


**Appendix C.3 :** Investigation of morphology of cells incubated with HER2-mAb containing in serum-free medium. (under 20x) (blue: DAPI; green: Phalloidin CruzFluor). (A) 40, (B)80, (C)120, and (D) 160 µg/mL HER2-mAb concentrations that cells treated.

**CURRICULUM VITAE**


**Name Surname** **: Hatice Eker**

**Place and Date of Birth** **: Konak, 24.03.1994**

**E-mail** **: ekerhtce@gmail.com**


**EDUCATION** **:**

- **B.Sc.** **:** 2017, Yıldız Technical University, Faculty of Chemical and Metalurgical, Bioengineering
- **B.Sc.** **:** 2018, Yıldız Technical University, Faculty of Arts and Sciences, Molecular Biology and Genetics

**PROFESSIONAL EXPERIENCE AND REWARDS:**

- 2019 Dec - Present Arcelik A.S., B&D, Project Engineer
- 2019 Mar - 2019 Dec World Medicine, R&D, Assistant Specialist
- 2017 Jul - 2018 Jun Arven Pharmaceuticals, R&D, Long Term Intern